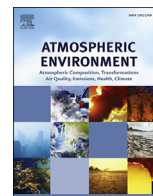




Contents lists available at ScienceDirect

Atmospheric Environment

journal homepage: www.elsevier.com/locate/atmosenv

Multi-year application of WRF-CAM5 over East Asia-Part I: Comprehensive evaluation and formation regimes of O₃ and PM_{2.5}



Jian He ^a, Yang Zhang ^{a,b,*}, Kai Wang ^a, Ying Chen ^a, L. Ruby Leung ^c, Jiwen Fan ^c,
Meng Li ^{d,e}, Bo Zheng ^e, Qiang Zhang ^{b,d}, Fengkui Duan ^e, Kebin He ^{b,d,e}

^a Air Quality Forecasting Laboratory, North Carolina State University, Raleigh, NC 27695, United States

^b Collaborative Innovation Center for Regional Environmental Quality, Beijing, 100084, PR China

^c Atmospheric Sciences and Global Change Division, Pacific Northwest National Laboratory, Richland, WA 99352, United States

^d Center for Earth System Science, Tsinghua University, Beijing, 100084, PR China

^e The School of Environment, Tsinghua University, Beijing, 100084, PR China

HIGHLIGHTS

- WRF-CAM5 can reproduce well observed meteorological variables and column mass abundances of CO, NO₂, and O₃.
- Large bias in cloud variable predictions due to uncertainties in representing clouds/ices and aerosol-cloud interactions.
- Large bias in surface concentrations due to uncertainties in emissions and vertical mixing.

ARTICLE INFO

Article history:

Received 9 February 2017

Received in revised form

5 June 2017

Accepted 8 June 2017

Available online 9 June 2017

Keywords:

Regional air quality

Regional climate change

Multi-year evaluation

O₃ and PM indicators

WRF-CAM5

East Asia

ABSTRACT

Accurate simulations of air quality and climate require robust model parameterizations on regional and global scales. The Weather Research and Forecasting model with Chemistry version 3.4.1 has been coupled with physics packages from the Community Atmosphere Model version 5 (CAM5) (WRF-CAM5) to assess the robustness of the CAM5 physics package for regional modeling at higher grid resolutions than typical grid resolutions used in global modeling. In this two-part study, Part I describes the application and evaluation of WRF-CAM5 over East Asia at a horizontal resolution of 36-km for six years: 2001, 2005, 2006, 2008, 2010, and 2011. The simulations are evaluated comprehensively with a variety of datasets from surface networks, satellites, and aircraft. The results show that meteorology is relatively well simulated by WRF-CAM5. However, cloud variables are largely or moderately underpredicted, indicating uncertainties in the model treatments of dynamics, thermodynamics, and microphysics of clouds/ices as well as aerosol-cloud interactions. For chemical predictions, the tropospheric column abundances of CO, NO₂, and O₃ are well simulated, but those of SO₂ and HCHO are moderately over-predicted, and the column HCHO/NO₂ indicator is underpredicted. Large biases exist in the surface concentrations of CO, NO_x, and PM₁₀ due to uncertainties in the emissions as well as vertical mixing. The underpredictions of NO lead to insufficient O₃ titration, thus O₃ overpredictions. The model can generally reproduce the observed O₃ and PM indicators. These indicators suggest to control NO_x emissions throughout the year, and VOCs emissions in summer in big cities and in winter over North China Plain, North/South Korea, and Japan to reduce surface O₃, and to control SO₂, NH₃, and NO_x throughout the year to reduce inorganic surface PM.

© 2017 Elsevier Ltd. All rights reserved.

* Corresponding author. Air Quality Forecasting Laboratory, North Carolina State University, Raleigh, NC 27695, United States.

E-mail address: yang_zhang@ncsu.edu (Y. Zhang).

1. Introduction

Atmospheric chemistry and aerosols play important roles in climate system perturbation. For example, changes in the amount and spatial distribution of tropospheric ozone (O₃) can affect the radiative forcing of climate change (Lacis et al., 1990; Forster et al.,

2007; Stevenson et al., 2013). Aerosols can affect climate system by directly scattering and absorbing radiation and indirectly through their roles as cloud condensation nuclei (CCN) and ice nuclei (IN) that influence cloud-radiation processes. Due to the non-linear relationship among chemistry, aerosols, clouds, and climate, it is important to simulate aerosol-cloud-climate interactions using 3-dimensional (3-D) climate models that represent such interactions. A number of online-coupled models at regional and global scales have been developed to study chemistry-climate interactions and feedback processes (Zhang, 2008). For example, the Weather Research and Forecasting (WRF) model is a regional atmospheric model that has been coupled online with chemistry (WRF/Chem, Grell et al., 2005; Y. Zhang et al., 2010; K. Wang et al., 2014), with the Community Multi-scale Air Quality model (WRF-CMAQ, Wong et al., 2012; Yu et al., 2014), and with the physics package of Community Atmosphere Model version 5 (WRF-CAM5, Ma et al., 2013; Lim et al., 2014; Y. Zhang et al., 2015a) to study chemistry-climate interactions and feedbacks on a regional scale. Global climate models such as the Gas, Aerosol, Transport, Radiation, General Circulation, Mesoscale, and Ocean Model (GATOC-GCMOM) of Jacobson (2001a, b), the Global-through-Urban WRF/Chem (GU-WRF/Chem, Y. Zhang et al., 2012a), and the Community Earth System Model with detailed chemistry (Lamarque et al., 2012; He and Zhang, 2014; Tilmes et al., 2015) are also developed to simulate these processes and feedbacks on a global scale.

Compared to global climate models that are mostly designed for their applications at coarse grid resolutions of $1^\circ \times 1^\circ$ to $5^\circ \times 5^\circ$ over the globe and may lack diurnal variation in emission sources, regional climate models can include more detailed treatments for physical and chemical processes and be applied at higher grid resolutions. The chemistry-climate feedbacks on a regional scale may be different from those on a global scale due to different characteristics of regional emissions and meteorological

phenomena. Several 3-D regional air quality and climate models have been applied over East Asia to study the meteorology/climate, air quality, and their interactions. Table 1 summarizes several examples of the regional air quality and climate models that have been applied over East Asia. These include CMAQ, WRF-CMAQ, WRF-Chem, WRF-CAM5, the Regional Climate Model version 3 (RCM3, Giorgi et al., 2002; Pal et al., 2007), the Regional Climate Chemistry Modeling System (RegCCMS, X.-Y. Wang et al., 2010), and the Regional Integrated Environmental Model System - Climate-chemistry-aerosol model (RIEMS-Chemaero, Han, 2010). These models have been applied over East Asia on various research topics including the impacts of anthropogenic emissions and resulting air pollutants on air quality (e.g., L.-T. Wang et al., 2010a, b; 2014; X.-Y. Wang et al., 2010; Y. Zhang et al., 2011, 2015b, 2016a), air pollution export (e.g., Lin et al., 2010), aerosol direct and/or indirect effects (e.g., Giorgi et al., 2002, 2003; T.-J. Wang et al., 2010, 2015; Zhuang et al., 2013; Liu et al., 2016), dust emissions and resulting climate impacts (e.g., K. Wang et al., 2012; Han et al., 2012, 2013; D. F. Zhang et al., 2009), aerosol activation (e.g., Y. Zhang et al., 2015a), new particle formation (e.g., Cai et al., 2015), and ice nucleation (e.g., Chen et al., 2015; Y. Zhang et al., 2015b). Among those applications, some of the models do not include the interactions between meteorology/climate and chemistry (e.g., MM5-CMAQ, one way WRF-CMAQ), whereas other models do (e.g., WRF-Chem, WRF-CAM5, RegCM, RegCM3, and RIEMS-Chemaero). While WRF-Chem, WRF-CAM5, and RIEMS-Chemaero provide a comprehensive representation of atmospheric aerosols, RegCM and RegCM3 include simplified aerosol treatments that predict only a few aerosol species such as sulfate, carbonaceous aerosols, and dust. All models except for WRF-CAM5 account for the interactions of aerosol with mix-phase and convective clouds. Further, all applications except for Giorgi et al. (2002) and D. F. Zhang et al. (2009) focus on short-term episodic simulations of specific processes. Giorgi et al. (2002)

Table 1
Regional air quality and climate models applied over east Asia.

Applications	Models ^a	Simulation Length	References
Anthropogenic emissions and air quality	MM5-CMAQ	Four-month (Jan, Apr, Jul, Oct) for 2005 and 2010	L.-T. Wang et al. (2010a, 2010b)
	MM5-CMAQ	Four-month (Jan., Apr., Jul., Oct., 2008)	Liu et al. (2010a, b)
	WRF-Chem	Jul., 2001	X.-Y. Wang et al. (2010)
	WRF-Chem	Two-month (Jan.-Feb., 2013)	L.-T. Wang et al. (2014)
Air pollution export	WRF-Chem	Four-month (Jan., Apr., Jul., Oct., 2005)	Y. Zhang et al. (2016a, 2016b)
	WRF-Chem, WRF-CMAQ	March, 2001	Lin et al. (2010)
Aerosol direct and indirect effects	RegCM,	Five-year (1993–1997)	Giorgi et al. (2002, 2003)
	WRF/Chem	Jul., 2001	X.-Y. Wang et al. (2010),
	RegCCMS	Thirteen-month (Nov. 2005–Dec., 2006)	Zhuang et al. (2013),
	RegCCMS	2000–2010	Wang et al. (2015)
Dust emission and climate impacts	WRF/Chem-MADRID	Four months (Jan., Apr., Jul., Oct., 2008)	Liu et al. (2016)
	WRF-CMAQ	Apr, 2001	K. Wang et al. (2012)
	RIEMS-Chemaero	Mar., 2010	Han et al. (2012, 2013)
	RegCM3	Nov.-Jun., 1997–2006	D. F. Zhang et al. (2009)
Aerosol activation	WRF-CAM5	Two full years (2005, 2010)	Y. Zhang et al. (2015a)
	WRF/Chem	Four months (Jan., Apr., Jul., Oct., 2001)	Cai et al. (2015),
New particle formation			
Ice nucleation	WRF-CAM5	Two full years (2006, 2011)	Chen et al. (2015), Y. Zhang et al. (2015b)
Chemistry-climate interactions, aerosol direct/indirect effects, chemical indicators, interannual variability	WRF-CAM5	Six full years (2001, 2005, 2006, 2008, 2010, 2011)	This work

^a MM5-CMAQ: the Fifth-Generation Mesoscale Model – the Community Multi-scale Air Quality (Byun and Schere, 2006); WRF-Chem: the Weather Research and Forecasting Model with Chemistry (Grell et al., 2005); WRF-CMAQ: the Weather Research and Forecasting Model with Chemistry – the Community Multi-scale Air Quality; RegCM3: the Regional Climate Model version 3 (Giorgi et al., 2002); RegCM3: the Regional Climate Model version 3 (Giorgi et al., 2002; Pal et al., 2007); RegCCMS: the Regional Climate Chemistry Modeling System (X.-Y. Wang et al., 2010); WRF/Chem-MADRID, the Weather Research and Forecasting Model with Chemistry from the Model of Aerosol Dynamics, Reaction, Ionization, and Dissolution (Y. Zhang et al., 2004); RIEMS-Chemaero, the Regional Integrated Environmental Model System - Climate-chemistry-aerosol model (Han, 2010); WRF-CAM5: the Weather Research and Forecasting Model with Chemistry – the Community Atmospheric Model version 5 (Ma et al., 2013).

performed a 5-year simulation of 1993–1997 using RegCM over East Asia to estimate the direct effects of sulfate and soot particles. Their model did not simulate natural aerosols such as mineral dust and biogenic aerosol and other anthropogenic aerosols such as carbon aerosols; it also did not account for aerosol indirect effects. While D. F. Zhang et al. (2009) applied RegCM3 for 8-month (Nov.–Jun.) during a 10-yr period (1997–2006), they simulated only the direct and semi-direct effects of dust. None of the above studies has examined the long-term regional air quality, climate, and their interactions, as well as their interannual variability over East Asia using online-coupled chemistry-climate models that simulate nearly all major anthropogenic and natural aerosols and also include both aerosol direct and indirect effects. On the other hand, Yahya et al. (2017) showed that including chemistry feedbacks into radiation and cloud microphysics improved model performance of radiation variables.

In this work, a regional climate model, WRF-CAM5, is applied over East Asia for multi-year simulation. The objectives are to evaluate the model's capability in reproducing long-term regional air quality, climate, and their interactions, examine interannual variability of meteorology, emissions, and the resulting concentrations, and estimate the relative importance of direct and indirect effects of anthropogenic aerosols and their interannual variability. WRF-CAM5 includes the CAM5 physics parameterizations used in the standalone global atmospheric model, CAM5. The application and evaluation of WRF-CAM5 in this work can therefore provide an assessment on the model's capability for long-term climate simulations and provide insights into the model biases and uncertainties as well as directions for future development and improvement. The results from this study will be presented as a sequence of two parts. Part I describes model configurations, application, and evaluation. Part II describes interannual variability, and relative importance of direct and indirect effects of anthropogenic aerosols.

2. Model configurations and methodology for evaluation and analysis

2.1. Model description and configurations

Due to the rapid growth of economy, China has become the largest contributors to global emissions for greenhouse gases such as carbon dioxide (CO₂), aerosol gaseous precursors such as sulfur dioxide (SO₂), nitrogen oxides (NO_x), ammonia (NH₃), and volatile organic compounds (VOCs), and aerosol species such as primary organic matters (POM). From 2000 to 2006, the anthropogenic NO_x emissions over mainland China increased from 3.8 Tg N yr⁻¹ (Q. Zhang et al., 2007) to 6.3 Tg N yr⁻¹ (Q. Zhang et al., 2009) and the anthropogenic SO₂ emissions over mainland China increased from 21.7 Tg to 33.2 Tg with an annual growth rate of 7.3% (Lu et al., 2010). The total SO₂ emissions decreased after 2006 mainly due to the wide application of flue gas desulfurization devices for power plants (Lu et al., 2010). In the past decade, to prevent the dramatic increase of emissions resulted from rapid growth in the economy and energy demand, the Chinese government implemented multi-phase emission control policies through the 10th Five Year Plan (FYP, 2001–2005) period, the 11th FYP (2006–2010) period, and the 12th FYP (2011–2015) period. The years of 2001, 2006, and 2011 are the first year of each FYP period and the years of 2005 and 2010 are the last year of the 10th and 11th FYP periods. The selection of those years for modeling in this study can thus represent the emission changes and assess the effectiveness of emission controls for the 10th and 11th FYP periods and the air quality for the start year of the 12th FYP period. The year of 2008 was selected before stringent emission controls were enforced to ensure good air quality for the 2008 Beijing Olympic Games (Witte et al., 2009). In

addition, another important event, the Shanghai World Expo 2010 was held during May to October, 2010 in Shanghai with similar stringent emission control measures (Hao et al., 2011). Six one-year additional sensitivity simulations are also conducted in 2001, 2006, and 2011 to estimate the overall aerosol effects, the relative importance of aerosol direct and indirect effects, as well as the interannual variability and trends of such effects in East Asia, which will be presented in Part II paper. Since 2001, 2006, and 2011 are the first year of each FYP period, the sensitivity simulations during these years will reflect the impacts of emission controls during the 10th and 11th FYP on air quality and its interactions with climate, relative to the baseline year of 2001.

WRF-CAM5 is a regional climate model that was developed by coupling WRF/Chem with the physics suite of CAM5 by the Pacific Northwest National Laboratory (PNNL). CAM5 is the atmospheric component of the Community Earth System Model version 1.0. WRF-CAM5 is designed to estimate the robustness of parameterizations in a multiscale framework (Ma et al., 2013). In this work, WRF-CAM5 is applied over East Asia for six years. In addition to baseline simulations for the six years, additional simulation are performed to separate direct, indirect, and total effects of anthropogenic aerosols, which will be described in Part II paper. Table 2 summarizes the model configurations used for baseline and sensitivity simulations in this work. Major physics options include the shortwave and longwave radiation scheme based on the Rapid Radiative Transfer Method for GCMs (RRTMG, Mlawer et al., 1997; Iacono et al., 2008), the planetary boundary layer (PBL) scheme of Bretherton and Park (2009), the Community National Centers for Environmental Prediction (NCEP), Oregon State University, Air Force, and Hydrologic Research Lab-NWS Land Surface Model (NOAH) (Chen and Dudhia, 2001; Ek et al., 2003), the microphysics scheme of Morrison and Gettelman (2008), the cumulus scheme based on Zhang and McFarlane (1995) with modifications by Song and Zhang (2011) as implemented in Lim et al. (2014), and the aerosol activation parameterization of Abdul-Razzak and Ghan (2000). The photolysis scheme is based on the Fast Troposphere Ultraviolet Visible (F-TUV) model (Madronich, 1987). The gas-phase chemistry is based on the Carbon-Bond mechanism version Z (CBMZ, Zaveri and Peters, 1999). The aqueous-phase chemistry is based on the simple sulfur oxidation mechanism of Barth et al. (2000). The aerosol module is based on the modal aerosol module with 3 lognormal modes (MAM3) of Liu et al. (2012). MAM3 simulates aerosol number and mass concentrations of major aerosol species, including black carbon (BC), mineral dust, sulfate (SO₄²⁻), ammonium (NH₄⁺), sea-salt, POM, and secondary organic aerosols (SOA). SOA is produced from a lumped SOA gas precursor based on the fixed mass yield approach.

All simulations are performed at a horizontal grid resolution of 36-km (with 164 grid cells in the X direction and 97 grid cells in the Y direction) and a vertical resolution of 23 layers from 1000 to 100 hPa. The meteorological initial and boundary conditions (ICs and BCs) are provided by the National Center for Environmental Predictions Final Analysis (NCEP-FNL). The meteorological fields are re-initialized every five days. The chemical ICs and BCs are based on the CMAQ modeling system (Binkowski and Roselle, 2003; Byun and Schere, 2006) and the Goddard Earth Observing System Atmospheric Chemistry Transport Model (GEOS-Chem). The anthropogenic emissions over mainland China for 2001, 2005, and 2008 are based on L.-T. Wang et al. (2010a) but with adjustments for the magnitudes and vertical distributions of emitted species described in Y. Zhang et al. (2015b, 2016a) based on the uncertainty factors in those emissions and model evaluation of an initial application using the original emissions. The anthropogenic emissions over mainland China for 2006, 2010, and 2011 are based on the Multi-resolution Emission Inventory for China (MEIC, <http://www.>

Table 2
WRF-CAM5 model components and Configurations.

Attribute	Model Configuration
Simulation period	2001, 2005, 2006, 2008, 2010, and 2011
Domain	East Asia
Resolution	Horizontal: 36-km (164 × 97); Vertical: 23 layers
Physical Options	
Shortwave/longwave radiation	The Rapid Radiative Transfer Method for GCMs (RRTMG, Mlawer et al., 1997 ; Iacono et al., 2008)
Planetary boundary layer (PBL)	The Bretherton-Park scheme (Bretherton and Park, 2009)
Land surface	The Community National Centers for Environmental Prediction (NCEP), Oregon State University, Air Force, and Hydrologic Research Lab-NWS Land Surface Model (NOAH) (Chen and Dudhia, 2001 ; Ek et al., 2003)
Microphysics	The Morrison 2-moment (Morrison and Gettelman, 2008)
Cumulus	The Zhang-McFarlane (Zhang and McFarlane, 1995) with modifications from Song and Zhang (2011) as implemented by Lim et al. (2014)
Aerosol activation	Abdul-Razzak and Ghan (Abdul-Razzak and Ghan, 2000)
Chemical Options	
Photolysis	The Fast Troposphere Ultraviolet Visible (F-TUV) (Madronich, 1987)
Gas-phase chemistry	The Carbon Bond mechanism version Z (CBM-Z) (Zaveri and Peters, 1999)
Aqueous-phase chemistry	Barth et al. (2000)
Aerosol module	The Modal aerosol model with three lognormal modes (MAM-3) (Liu et al., 2012)

[meicmodel.org](#); [He \(2012\)](#); [He et al., 2015](#)). The anthropogenic emissions over regions and countries outside China are based on L.-T. [Wang et al. \(2010a\)](#) for 2001, 2005, and 2008, and the Intercontinental Chemical Transport Experiment-Phase B (INTEX-B) emission inventory of Q. [Zhang et al. \(2009\)](#) for 2006, 2010, and 2011. The emission inventories of L.-T. [Wang et al. \(2010a\)](#) and MEIC are actually constructed by the same group. Both of them were developed using the same technology-based method, which estimates emissions for each source according to its fuel type, combustion/industrial process and control technology ([Zhang et al., 2007, 2009](#)). The changes of fuel contents and penetration of technologies for each source were tracked and the therefore emission trends were achieved in time series analysis. Hourly variations in these emissions are accounted for ([Huo et al., 2009](#)). The online emissions include biogenic emissions from the Model of Emissions of Gases and Aerosols from Nature (MEGAN) version 2 ([Guenther et al., 2006](#)), dust emissions based on a modified version of [Zender et al. \(2003\)](#) as implemented by [Wang et al. \(2012\)](#), and sea-salt emissions based on [Gong et al. \(2002\)](#).

2.2. Available measurements and evaluation protocols

A number of observational datasets from surface networks, satellites, and aircraft are used for model evaluation. They are summarized along with the variables to be evaluated in [Tables S1 and S2](#) in the supplementary material. The meteorological and radiative variables evaluated include temperature at 2-m (T2), specific humidity at 2-m (Q2), and wind speed at 10-m (WS10) from the National Climatic Data Center (NCDC); daily precipitation rate (precipitation) derived from the Global Precipitation Climatology Project (GPCP) and NCDC; outgoing longwave radiation (OLR), downwelling shortwave radiation (SWD), downwelling longwave radiation (LWD), shortwave cloud forcing (SWCF), and longwave cloud forcing (LWCF) retrieved from the Clouds and Earth's Radiant Energy System (CERES) Energy Balanced And Filled data product (CERES-EBAF); cloud condensation nuclei (CCN), cloud fraction (CF), cloud optical thickness (COT), precipitable water vapor (PWV), cloud liquid water path (LWP), and cloud ice water path (IWP) retrieved from the Moderate Resolution Imaging Spectroradiometer (MODIS); aerosol optical depth (AOD) from MODIS and Aerosol Robotic Network (AERONET); and cloud droplet number concentration (CDNC) from [Bennartz \(2007\)](#). Surface chemical concentrations evaluated include carbon monoxide (CO),

O₃, SO₂, nitrogen monoxide (NO), nitrogen dioxide (NO₂), particulate matter with diameter less than and equal to 2.5 μm and 10 μm (PM_{2.5} and PM₁₀, respectively) from mainland China, Hong Kong, Taiwan, Japan, and South Korea; PM_{2.5} components including sulfate (SO₄²⁻), ammonium (NH₄⁺), sodium (Na⁺) and chloride (Cl⁻) over a suburban site, Tsinghua University (THU), and a rural site, Miyun, in Beijing, China; major gaseous species (i.e., SO₂, NO₂, O₃, nitric acid (HNO₃), and ammonia (NH₃)) and aerosol species (i.e., PM₁₀, SO₄²⁻, NH₄⁺, Na⁺, and Cl⁻) at sites from the Acid Deposition Monitoring Network in East Asia (EANET). Among all surface photochemical indicators suggested by Y. [Zhang et al. \(2009\)](#), O₃/NO_x is the only indicator that can be calculated based on available observations, which is used for photochemical indicator evaluation. The PM indicators evaluated include the degree of sulfate neutralization based on molar ratio (DSN = ([NH₄⁺] + [NO₃⁻])/[SO₄²⁻], [Pinder et al. \(2008\)](#)), gas ratio (GR = ([NH₃] + [NH₄⁺] - 2 × [SO₄²⁻])/([NO₃⁻] + [HNO₃]), [Ansari and Pandis \(1998\)](#)), and adjusted gas ratio (AdjGR = ([NH₃] + [NO₃⁻])/[NO₃⁻] + [HNO₃]), [Pinder et al. \(2008\)](#)). Column concentrations are also evaluated, including tropospheric CO retrieved from the Measurements Of Pollution In The Troposphere (MOPITT), tropospheric NO₂, SO₂, and formaldehyde (HCHO) retrieved from the SCanning Imaging Absorption spectroMeter for Atmospheric CHartographY (SCIAMACHY), and tropospheric O₃ residual (TOR) retrieved from the Aura Ozone Monitoring Instrument in combination with Aura Microwave Limb Sounder (OMI/MLS).

Model evaluation protocol follows Y. [Zhang et al. \(2012b, 2015a\)](#). The evaluation is performed in terms of domain-wide performance statistics, the spatial distributions of meteorological variables including radiation and cloud parameters and chemical concentrations, the vertical distribution of CCN, the column abundances of major gases, and scatter and bar plots for surface concentrations. The performance statistics are calculated in terms of mean bias (MB), normalized mean bias (NMB), normalized mean error (NME), and correlation coefficient (R) (see their definitions in [Yu et al. \(2006\)](#) and [Zhang et al. \(2006\)](#)) based on 6-year annual averages and seasonal means. They are calculated separately for comparison using different observational networks. Following [Campbell et al. \(2015\)](#), surface O₃ and PM_{2.5} indicators are evaluated against surface observations over different networks, and column HCHO/NO₂ ([Martin et al., 2004](#)) indicator is also evaluated against SCIAMACHY satellite observations.

Variations of emissions, major meteorological and cloud/

radiative variables, chemical concentrations, and aerosol effects are discussed in this work through trend analysis and interannual variability comparisons. Profile comparisons are also conducted over five major cities (i.e., Beijing, Chengdu, Guangzhou, Shanghai, and Urumqi) to estimate the aerosol direct and indirect effects on meteorological predictions. Different from other cities that are moderately to heavily polluted, Urumqi does not have major anthropogenic sources, thus representing background concentrations.

3. Model evaluation

3.1. Meteorological predictions

Table 3 summarizes the domain-mean performance statistics based on six year averaged results. Fig. 1 shows the spatial distributions of annual mean MBs of T2, Q2, WS10, and precipitation against the NCDC dataset based on 6-year results and Fig. 2 shows the bar plots of seasonal mean NMBs of model predictions based on 6-year results. As shown in Fig. 1, T2 is slightly too cold except along the southern coast of South Korea and the eastern and southern coast of Japan, which can be attributed to the relatively coarse grid resolution (i.e., 36 km) that cannot accurately resolve the coastline and/or coastal processes such as land-sea breezes. The 6-year mean MB is $-1.0\text{ }^{\circ}\text{C}$ and NMB is -7.2% for T2. As shown in Fig. 2, a general cold bias occurs in all seasons. Among the four seasons, the winter MB for T2 is the smallest (i.e., $-0.5\text{ }^{\circ}\text{C}$) and the summer MB for T2 is the largest (i.e., $-1.4\text{ }^{\circ}\text{C}$), which is likely due to the limitation of WRF-CAM5 in capturing the mountainous terrain at 36-km resolution and/or reproducing the observed snow cover and its rate of melting. Consequently, Q2 is largely overpredicted over southeastern coast of mainland China and South Korea and Japan, despite it is slightly underpredicted over inland China. The spatial correlation coefficients between observations and simulations for T2 and Q2 are 0.98 and 0.98 over the entire domain, indicating the model can generally capture the spatial and temporal distributions of T2 and Q2. WS10 is relatively well predicted over mainland China but significantly overpredicted over North and South Korea and Japan, which is likely due to uncertainties in predicting surface roughness and surface drag in the mountainous terrain by the coarse grid resolution. Precipitation are relatively well predicted over

mainland China but overpredicted over Japan, Myanmar, and the southern boundaries much more often in summers than in winters, indicating that the overpredictions in total precipitation are mainly caused by overpredictions in convective precipitation over these regions. In WRF-CAM5, the deep convection scheme is based on Zhang and McFarlane (1995) with modifications from Song and Zhang (2011), which was originally designed for global applications at a coarse resolution. For regional application at 36-km in this work, precipitation biases could exist because the convection closure works well only for coarse resolution grids. Overall, larger biases are found over the Korean Peninsula and Japan with complex terrain and coastline and in western and southwestern China, which are marked by higher elevation.

Fig. 3 shows the spatial distributions of 6-year average values of major meteorological and radiative variables from satellite retrievals and WRF-CAM5 simulations. Compared to GPCP data, precipitation is slightly overpredicted, with an NMB of 12.1%. As shown in Fig. 3, precipitation is well predicted over land, but overpredicted over remote oceanic areas. Compared to MODIS data, cloud variables such as CF and PWV are well predicted, with NMBs of -9.7% and -0.4% , respectively, despite slightly underprediction or overprediction over some regions (see Fig. 3). The overpredictions of precipitation and CF over the ocean may be attributed to uncertainties in the convection and cloud parameterizations. The simulated CCN at supersaturation of 0.5% (CCN5) over land cannot be evaluated because MODIS does not contain CCN5 over land. CCN5 over ocean is moderately underpredicted, with an NMB of -35.8% , especially along coastal zones. The underpredictions of CCN5 can be attributed to the limitations in the current model treatments of cloud microphysics and aerosol-cloud interactions as well as underpredictions of aerosol concentrations. Fig. 4 shows the vertical distributions of averaged CCN in Beijing over the period of July–September 2008. Compared to the aircraft measurements obtained at supersaturation of 0.3%, the simulated CCN at supersaturation of 0.2% is slightly lower and that at supersaturation of 0.5% is higher (particularly at altitudes $< 1600\text{ m}$) (note that WRF-CAM5 does not calculate CCN at supersaturation of 0.3%), but within the uncertainty range of the aircraft measurements. In general, WRF-CAM5 can represent relatively well the observed vertical distribution of CCN over Beijing.

Cloud variables such as CDNC, COT, LWP, and IWP are also

Table 3
6-yr average performance statistics for meteorological, radiative, and cloud variables from WRF-CAM5 simulations.

Variable	Dataset ^a	6-yr average							
		Number	Mean Obs.	Mean Sim.	MB	NMB,%	NME,%	RMSE	R
T2, $^{\circ}\text{C}$	NCDC	64146	13.6	12.6	-1.0	-7.2	14.5	2.7	0.98
Q2, g kg^{-1}	NCDC	41381	7.93	7.97	0.04	0.5	10.2	1.1	0.98
WS10, m s^{-1}	NCDC	48130	3.1	3.4	0.3	10.2	31.8	1.3	0.5
Precipitation, mm day^{-1}	NCDC	62152	2.6	3.0	0.4	13.8	64.6	3.3	0.6
	GPCP	964656	2.8	3.2	0.3	12.1	64.9	3.2	0.6
CF	MODIS	964656	0.64	0.58	-0.06	-9.7	22.3	0.2	0.7
PWV, cm	MODIS	964609	2.21	2.20	-0.01	-0.4	10.7	32.6	0.98
CCN _{0.5} (ocean), cm^{-2}	MODIS	346468	7.6×10^8	4.9×10^8	-2.7×10^8	-35.8	48.6	8.0×10^8	0.6
CDNC, cm^{-3}	Bennartz (2007)	359521	141.3	115.2	-26.2	-18.5	45.6	85.0	0.5
COT	MODIS	964646	16.2	8.6	-7.6	-47.1	55.5	10.3	0.6
LWP, g m^{-2}	MODIS	964630	109.5	50.9	-58.6	-53.5	58.5	73.6	0.7
IWP, g m^{-2}	MODIS	964251	241.3	9.4	-231.9	-96.1	96.1	259.0	0.2
AOD	MODIS	883727	0.3	0.2	-0.1	-36.7	52.0	0.2	0.5
	AERONET	8615	0.4	0.3	-0.2	-43.1	66.3	0.5	0.4
OLR	CERES	964656	235.8	236.8	1.0	0.4	2.8	9.5	0.9
SWD, W m^{-2}	CERES	964656	181.7	203.1	21.4	11.8	13.5	30.6	0.9
LWD, W m^{-2}	CERES	964656	324.9	315.9	-8.9	-2.8	3.5	15.5	0.99
SWCF, W m^{-2}	CERES	964656	-52.9	-43.7	-9.2	-17.4	28.0	19.7	0.9
LWCF, W m^{-2}	CERES	964656	29.4	19.0	-10.4	-35.3	38.0	13.7	0.8

^a NCDC: National Climatic Data Center; GPCP: Global Precipitation Climatology Project; MODIS: Moderate Resolution Imaging Spectroradiometer; AERONET: Aerosol Robotic Network; CERES: Clouds and Earth's Radiant Energy System.

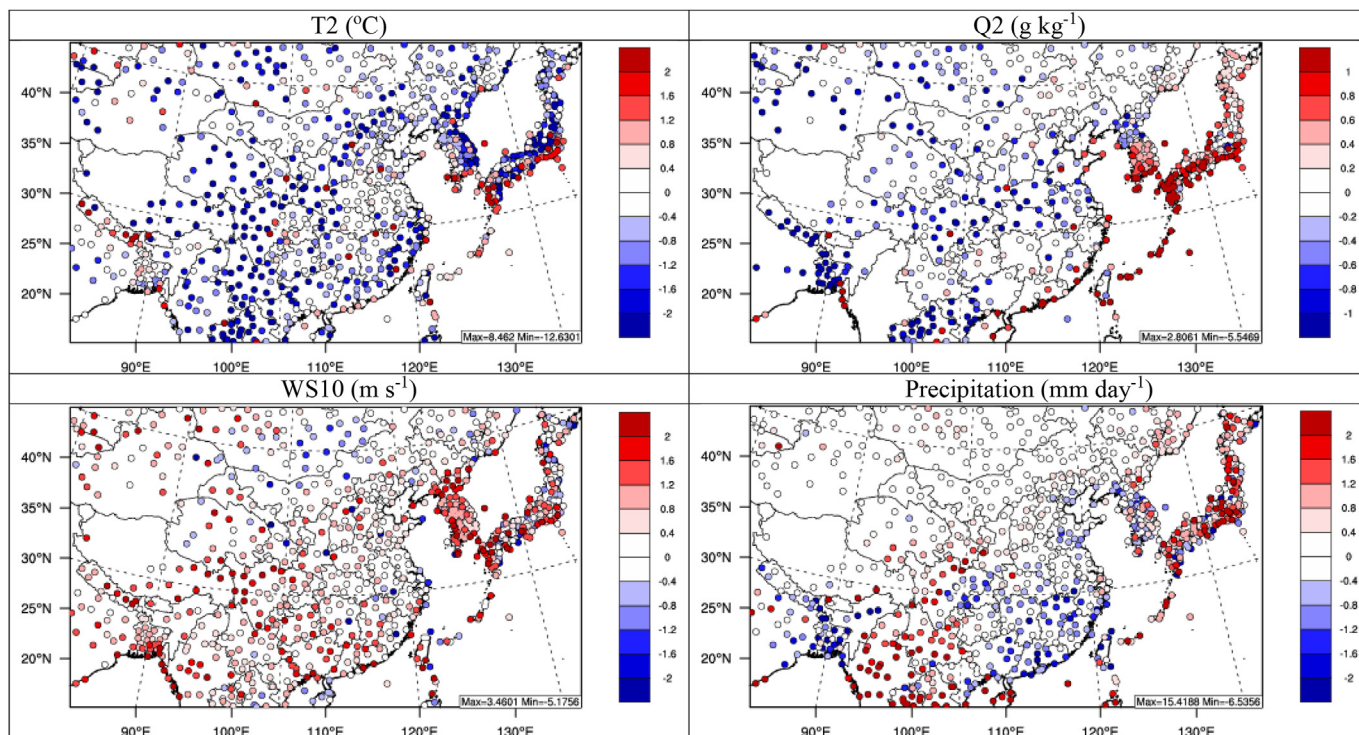


Fig. 1. Spatial distributions of 6-year mean MBs of temperature at 2-meter (T2), specific humidity at 2-meter (Q2), wind speed at 10-meter (WS10), and precipitation at NCDG sites.

moderately underpredicted in all seasons, with annual mean NMBs of -96.1% to -18.5% . The underpredictions of these cloud variables can be due in part to uncertainties in the cloud thermodynamics and dynamics treatment, the ice microphysics, the aerosol activation parameterization, and the satellite retrievals, as well as the underpredictions of aerosols as discussed in Section 3.2. For example, the uncertainties in ice microphysics have been reported in several studies (e.g., Gilmore et al., 2004; McFarquhar et al., 2006; Morrison and Grabowski, 2008). Y. Zhang et al. (2015a) incorporated an advanced aerosol activation scheme into WRF5-CAM5 to improve CDNC predictions, and Y. Zhang et al. (2015b) conducted sensitivity simulations with different ice nucleation schemes that can result in different predicted nucleated ice crystal number concentrations by over 100% in spring. These results indicate the uncertainties in the treatments for ice nucleation and aerosol activation in the physics options used in this work. The domain-wide underpredictions of total water path LWP+IWP) could be due in part to the overestimations of autoconversion of cloud water to rain droplets, leading to the overpredictions of precipitation. In addition, such underpredictions suggest possibly dry bias in thermodynamics, which is a typical problem of NCEP FNL data over mid-latitudes. Large biases also exist in the MODIS retrievals of cloud parameters. For example, uncertainties exist in the MODIS-derived LWP, which could be attributed to several factors including neglecting cloud vertical stratification and the effect of absorbing aerosols under polluted conditions with high aerosol loading, errors in cloud top effective radius retrievals, and the assumption of vertical homogeneity (Seethala and Horváth, 2010). The underpredictions in CDNC and LWP can propagate to the COT predictions, resulting in underpredictions of COT. AOD is also moderately to largely underpredicted, with NMBs of -50.1% (winter) to -30.6% (spring), leading to the net 6-year average NMB of -36.7% . As shown in Fig. 3, AOD is underpredicted especially over eastern China. The underpredictions of AOD are likely due to uncertainties in the anthropogenic emissions, the use of a coarse

grid resolution, the vertical mixing scheme, the online dust emission module, the online sea-salt emission module, and satellite retrievals. For example, Chu et al. (2005) found that AOD is overestimated by MODIS over dust regions due to the nonsphericity effects associated with dust, and Wang et al. (2007) found that AOD is overestimated by MODIS over desert, arid regions, and plateaus due to errors in the surface reflectance estimations.

Radiative variables such as LWD and OLR are well predicted, with NMBs of -2.8% and 0.4% , respectively, and correlation coefficients of 0.99 and 0.92, respectively. Due to the underpredictions of cloud variables (e.g., COT, LWP, IWP, and CDNC), SWCF and LWCF are also underpredicted, with NMBs of -30.0% (winter) to -6.8% (summer) and -45.0% (winter) to -30.0% (summer), respectively, leading to the net 6-year average NMBs of -17.4% and -35.3% , respectively. The underpredictions of SWCF and LWCF could possibly be due in part to the uncertainties in cloud treatments as well as inaccurate predictions in aerosol concentrations as shown in He and Zhang (2014). As a result, SWD is slightly-to-moderately overpredicted, with NMBs of 8.2% (fall) to 16.8% (winter), leading to the net 6-year average NMB of 11.8% .

3.2. Chemical surface predictions

Fig. 5 shows the scatter plots for major chemical species over mainland China, Hong Kong, Taiwan, South Korea, and Japan, and Fig. 6 compares the observations and simulations for major gases and aerosol species over the EANET sites. The 6-yr average observed and simulated species concentrations in six major cities in Mainland China, Japan, and South Korea are shown in Fig. S1. As shown in Fig. 5, the 6-year average surface concentration of CO is moderately underpredicted over Hong Kong, Taiwan, South Korea, and Japan (with NMBs of -58.5% to -38.1%). As shown in Fig. 2, the seasonal-mean surface concentration of CO is moderately underpredicted, with NMBs of -38.7% (fall) to -47.3% (winter). The underpredictions of CO concentrations can be due in part to the

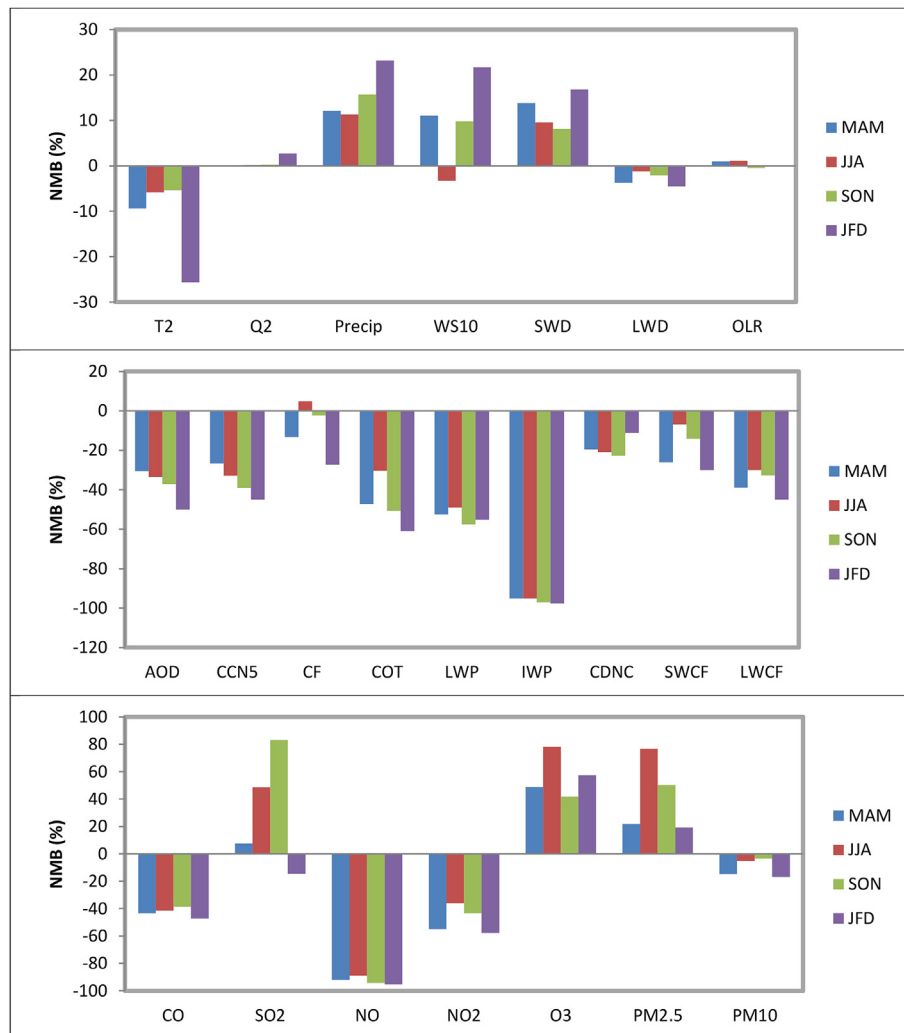


Fig. 2. Bar plots of seasonal-mean normalized mean bias (NMB, %) for major meteorological/cloud variables and chemical species predictions for four seasons during the six simulated years. Spring, March–April–May (MAM); summer, June–July–August (JJA); fall, September–October–November (SON); winter, January–February–December (JFD). The observational data for T2, Q2, Precipitation, and WS10 are from the National Climatic Data Center (NCDC), the observational data for SWD, LWD, OLR, LWCF, and SWCF are from the Clouds and Earth’s Radiant Energy System (CERES) Energy Balanced And Filled data product (CERES-EBAF); the observational data for AOD, CCN5, CF, COT, LWP, and IWP are from the Moderate Resolution Imaging Spectroradiometer (MODIS), and the observations for chemical species are from mainland China, Hong Kong, Taiwan, South Korea, and Japan.

uncertainties in vertical distribution of CO emissions and the possibly overpredictions in the vertical transport due to convection scheme of Bretherton and Park (2009) and Zhang and McFarlane (1995). As shown in Fig. 5, the surface concentration of SO₂ is moderately underpredicted over mainland China, Taiwan, South Korea, and Japan (with NMBs of –55.8% to –15.2%), whereas it is largely overpredicted over Hong Kong (with an NMB of 119.9%). As shown in Fig. 2, the seasonal-mean surface concentration of SO₂ is slightly to largely overpredicted with NMBs of 7.5% (spring) to 83.1% (fall), but underpredicted in winter with an NMB of –14.5%. The overpredictions of the seasonal-mean SO₂ concentrations over all surface networks are dominated by the large overpredictions at the Hong Kong sites (see Table 4). Similar overpredictions of SO₂ are also found in all seasons and annual mean based on 6-year simulations over the EANET sites (see Fig. 6) with a 6-year average NMB of 87.1%. The biases in SO₂ concentration predictions are likely due to the uncertainties in the anthropogenic SO₂ emissions and the use of a coarse grid resolution. For example, Hong Kong is located in only one grid cell in the domain. The use of a coarse grid resolution fails to capture the fine-scale details for Hong Kong, resulting in large biases in the chemical predictions at this site. The surface

concentrations of NO and NO₂ are moderately to largely underpredicted over major cities in mainland China, Hong Kong, Taiwan, South Korea, and Japan sites (see Fig. S1), with NMBs of –95.4% and –57.7% in winter and NMBs of –88.9% and –36.2% in summer, respectively. The underpredictions of NO_x concentrations are mainly due to the uncertainties in the NO_x emissions (Y. Zhang et al., 2016a). Similar underpredictions of NO₂ are also found over the EANET sites in all seasons, with a 6-year average NMB of –48.2%. As shown in Fig. 2, the surface O₃ concentrations over all surface networks are overpredicted, with NMBs of 48.8% (fall) to 78.2% (summer), which is mainly due to underpredictions of O₃ titration caused by the underpredictions of NO concentrations. As shown in Fig. 5, the overpredictions of O₃ concentrations are dominated by the overpredictions of O₃ concentrations at the Hong Kong site, whereas O₃ concentrations are relatively well predicted over Taiwan, Japan, and South Korea, despite the underpredictions of O₃ concentrations at a few sites in South Korea. Unlike the O₃ performance over Hong Kong, Taiwan, Japan, and South Korea sites, the surface O₃ concentrations are well predicted over the EANET sites in fall and winter but higher biases occur for JJA and MAM (with NMBs of 24.1% and –13.2%), with a 6-year average NMB of

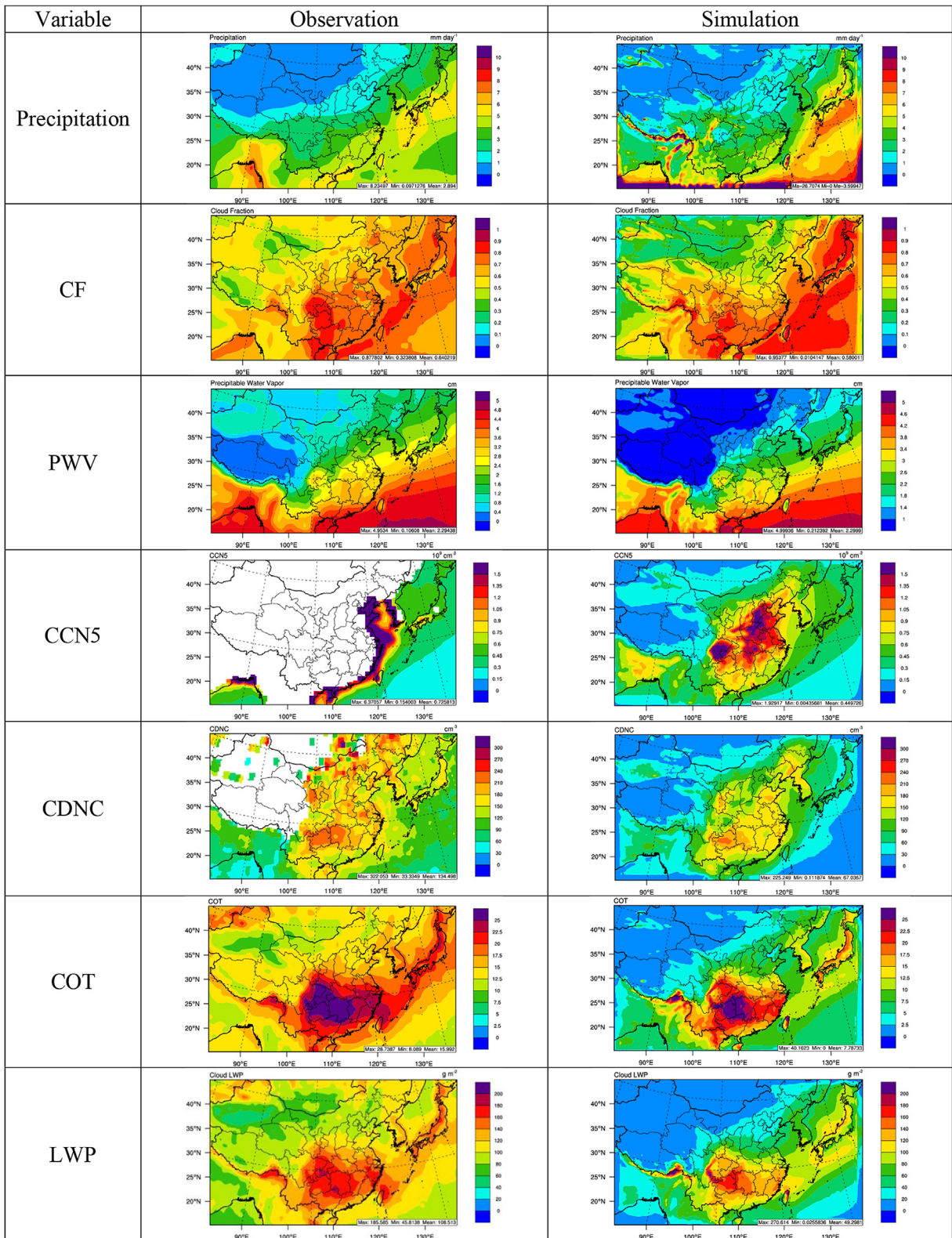


Fig. 3. Spatial distributions of 6-year average values of meteorological and cloud variables from satellite retrievals and WRF-CAM5 simulations. Note that a different scale is used for obs and sim IWP.

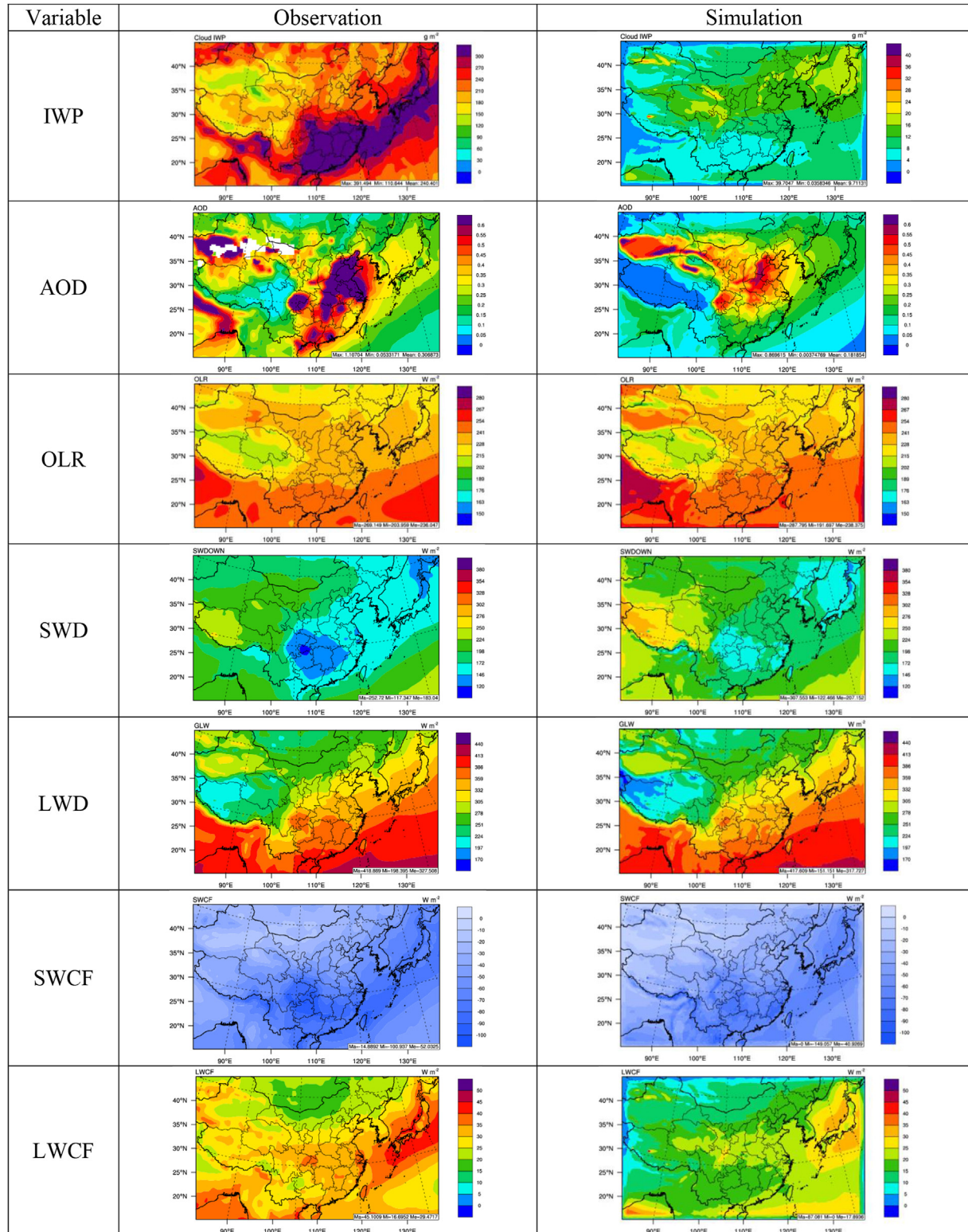


Fig. 3. (continued).

0.002%. As shown in Fig. 6, the surface HNO_3 and NH_3 concentrations are moderately to largely overpredicted over the EANET sites, with NMBs of 129.0% and 52.7%, respectively. The overpredictions of surface HNO_3 and NH_3 concentrations are mainly due to missing treatments for gas-particle partitioning between HNO_3 and NO_3^-

and NH_3 and NH_4^+ in MAM3 as explained in He and Zhang (2014) and Yu et al. (2005) as well as uncertainties in NO_x and NH_3 emissions.

As shown in Fig. 2, surface $\text{PM}_{2.5}$ concentrations are moderately to largely overpredicted, with seasonal-mean NMBs of 19.4%

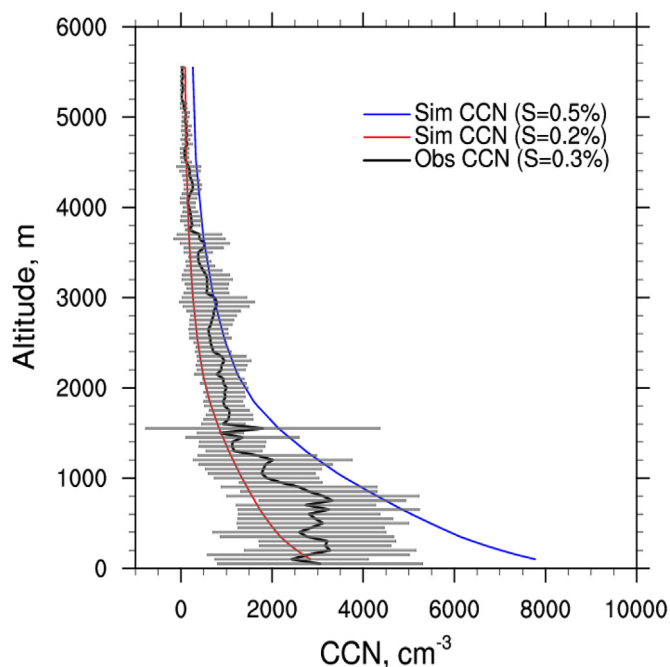


Fig. 4. Vertical distributions of average values of CCN in Beijing over the period of July–September 2008 from aircraft measurements and WRF-CAM5 simulations. CCN obs. data are taken from Zhang et al. (2011).

(winter) to 76.7% (summer). The observed $PM_{2.5}$ concentrations are only available over Hong Kong and Taiwan (See Fig. 5). The over-predictions of $PM_{2.5}$ concentrations are likely due to the use of a coarse grid resolution and uncertainties in the emissions such as aerosol gaseous precursors (e.g., SO_2 and NH_3) and primary aerosols (e.g., SO_4^{2-} , BC, and OC) over these regions. Unlike $PM_{2.5}$, surface PM_{10} concentrations are underpredicted with seasonal-mean NMBs of -16.9% (winter) to -3.4% (fall). The observed PM_{10} concentrations are available over Hong Kong, Taiwan, South Korea, and Japan, and can be derived from API mainland China. As shown in Fig. 5, PM_{10} concentrations are underpredicted over all these sites, which is mainly due to the uncertainties in the anthropogenic emissions for aerosol gaseous precursors (e.g., SO_2 , NO_x , and NH_3), primary aerosols (e.g., SO_4^{2-} , BC, and OC), and online emission modules (e.g., dust and sea-salt). Fig. 7 shows the 6-yr average observed and simulated concentrations of PM at Tsinghua (THU) and Miyun sites in Beijing, China and Fig. S2 shows the scatter plots of $PM_{2.5}$ and its components at the Tsinghua (THU) and Miyun sites in Beijing, China. As shown in Fig. 7 and Fig. S2, surface $PM_{2.5}$ concentrations are relatively well predicted at the Miyun site, with an NMB of -4.8% , whereas they are moderately underpredicted at the THU site, with an NMB of -24.6% . The underpredictions of $PM_{2.5}$ are due to the underpredictions of the PM components. As shown in Fig. 7, the surface concentrations of SO_4^{2-} and NH_4^+ are underpredicted at THU and Miyun sites, with NMBs of -40.9% and -81.2% at THU and -23.5% and -74.6% at Miyun, respectively. Similarly shown in Fig. 6, the surface concentrations of SO_4^{2-} and NH_4^+ are underpredicted at the EANET sites, with NMBs of -55.8% and -69.2% , respectively. The underpredictions of surface SO_4^{2-} and NH_4^+ can be attributed to insufficient conversion of SO_2 and NH_3 to SO_4^{2-} and NH_4^+ , respectively, as the model shows overpredictions of the concentrations of SO_2 and NH_3 at the EANET sites (Fig. 6). In addition, MAM3 used in WRF-CAM5 assumes that SO_4^{2-} and NH_4^+ exist as ammonium bisulfate (NH_4HSO_4), which may introduce some uncertainties because it does not consider other types of sulfate salts such as ammonium sulfate. The surface concentrations

of Na^+ and Cl^- are largely underpredicted at the THU and Miyun sites, with NMBs of -97.6% and -98.9% at THU, and -97.7% and -96.8% at Miyun, respectively. Similar performances are also found over the EANET sites, where the surface concentrations of Na^+ and Cl^- are underpredicted with 6-year average NMBs of -42.6% and -32.1% , respectively. The underpredictions of Na^+ and Cl^- are mainly due to the uncertainties in the sea-salt emissions and missing sources for Cl^- such as anthropogenic emissions. In addition, similar to SO_4^{2-} and NH_4^+ , Na^+ and Cl^- are treated as one species (i.e., sea-salt, NaCl) in the model. In reality, the sources of Cl^- are not only from sea-salt but also from the partitioning between HCl and Cl^- . However, the model does not simulate the gas-aerosol partitioning for volatile species, which is another source of uncertainty for gas/aerosol predictions. He and Zhang (2014) implemented an advanced inorganic aerosol thermodynamic module, ISORROPIA II of Fountoukis and Nenes (2007), into CEM/CAM5 to simulate the gas-aerosol partitioning for HNO_3/NO_3^- , NH_3/NH_4^+ , and HCl/ Cl^- . Their results show that with the explicit aerosol thermodynamic treatments, CAM5 improves the predictions of NH_4^+ , NO_3^- , and Cl^- significantly. Therefore, missing important aerosol processes in the model can partly explain the large biases in gas and aerosol predictions.

3.3. Chemical column concentrations

As shown in Table 4, the column concentrations of gaseous species such as CO, NO_2 , and TOC are relatively well predicted, with 6-year average NMBs of 5.5%, -6.9% , and 10.0%, respectively. However, as discussed above, surface CO and NO_2 are moderately underpredicted, indicating the model uncertainties in the vertical transport due to model treatment in the convection as well as uncertainties in the vertical distribution of these emissions. Column SO_2 concentrations are moderately overpredicted, with a 6-year average NMB of 27.0%. The overpredictions of column SO_2 concentrations can be due in part to the uncertainties in the vertical distribution of SO_2 emissions (Y. Zhang et al., 2016a) and uncertainties in the satellite retrievals. For example, Lee et al. (2009) reported an overall error in the annual SO_2 retrievals of 45–80% over polluted regions, especially over eastern China. In addition, the uncertainty in the total energy consumption could lead to uncertainty in the emission estimations as shown in Hong et al. (2017). For example, the overestimations of coal consumption are likely to overestimate the SO_2 emissions, and therefore lead to overpredict SO_2 . Column HCHO concentrations are also moderately overpredicted, with 6-year average NMBs of 19.6%. The overpredictions of column HCHO concentrations are due in part to the uncertainties in the HCHO emission and its precursor emissions (e.g., isoprene), chemical productions and removals, as well as uncertainties in the satellite retrievals (De Smedt et al., 2008).

Figs. 8 and 9 compare the simulated 6-year average column concentrations with those from satellite retrievals in summer and winter. As shown in Fig. 8, in summer, compared to MOPITT data, the model predicts higher domain averaged column CO by 2.9×10^{17} molecules cm^{-2} (or by 18.0%), especially over North China Plain. The overpredictions of column CO concentrations and underpredictions of surface CO concentrations are likely due to uncertainties in the total CO emissions as well as vertical distribution of CO emissions. Compared to SCIAMACHY data, the model predicts higher column SO_2 by 1.5 Dobson Units (DUs) over North China Plain, but lower column SO_2 by 0.1–0.4 DU over the western domain and ocean. This is likely due to uncertainties in the spatial and vertical distributions of SO_2 emissions. Column NO_2 concentrations and TOC are relatively well predicted in summer, despite their slight underpredictions over northern China. Compared to SCIAMACHY data, domain averaged column HCHO concentrations

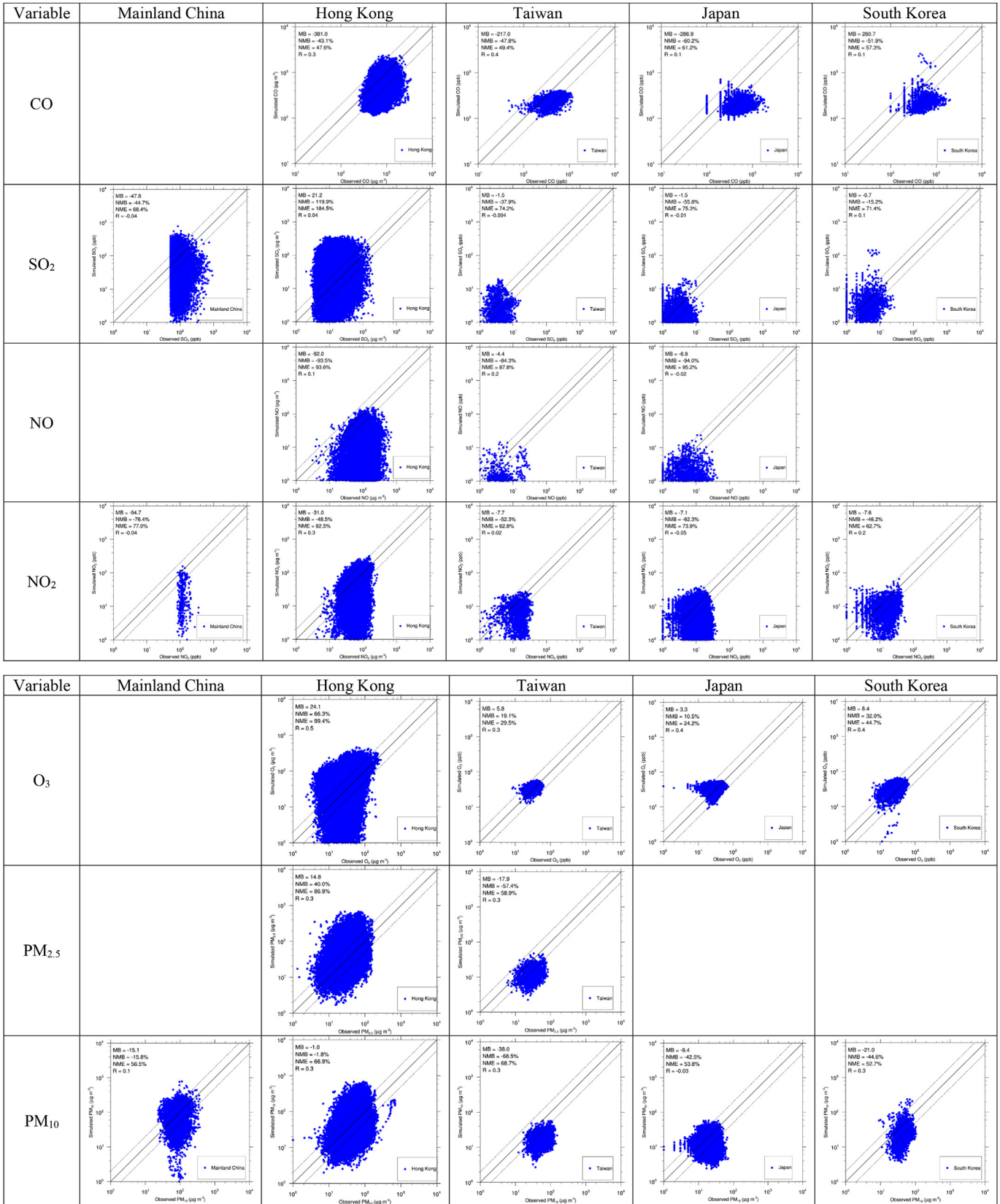


Fig. 5. Scatter plots of 6-yr average observed and simulated species concentrations in Mainland China, Hong Kong, Taiwan, Japan, and South Korea. Blank areas for some species at some sites indicate no observations were available.

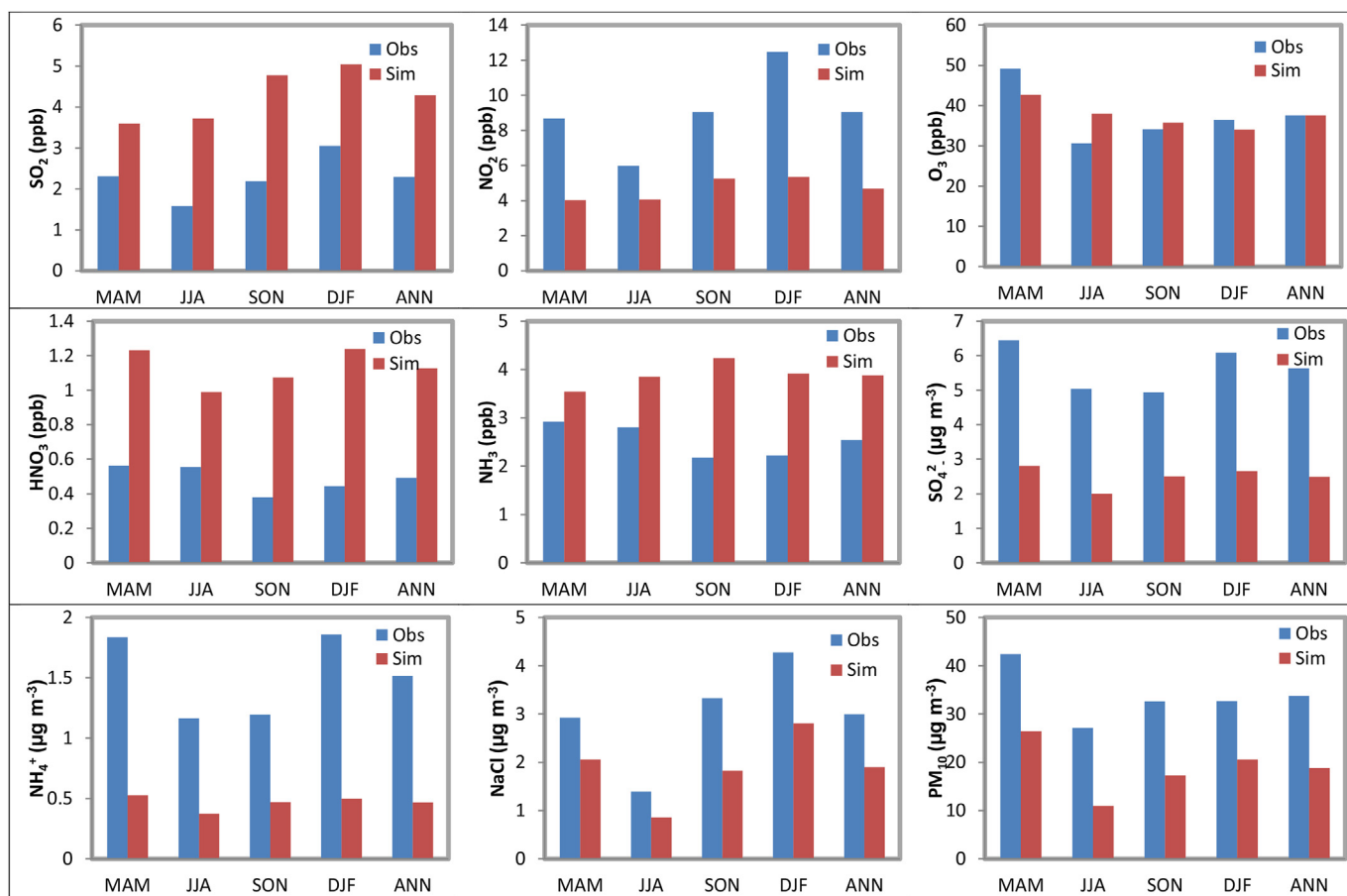


Fig. 6. Comparison of observed and simulated surface chemical concentrations over EANET sites for 6-year average March–April–May (MAM), June–July–August (JJA), September–October–November (SON), December–January–February (DJF), and annual average (ANN).

are overpredicted by 1.6×10^{15} molecules cm^{-2} (or by 25.6%), especially over eastern China, South Korea, and Japan. Similarly, as shown in Fig. 9, in winter, the model predicts higher domain averaged column abundances of CO, SO_2 , and HCHO, by 8.4×10^{16} molecules cm^{-2} (or by 4.1%), 0.13 DU (or by 54.4%), and 1.7×10^{14} molecules cm^{-2} (or by 0.3%), especially over eastern China. However, the model predicts lower domain averaged column NO_2 by 3.5×10^{14} molecules cm^{-2} (or by 10.4%), especially over North China Plain. Higher SWD predicted in winter against satellite observations can result in higher photolysis of NO_2 to produce more O_3 . As a result, the model predicts higher domain averaged TOC by 6.2 DUs (or by 24.0%). On the other hand, Ziemke et al. (2006) reported an error of $\pm(4-5)$ DUs in the OMI TOC retrievals, indicating the overpredictions of TOC can also be due in part to the uncertainties in the OMI retrievals.

3.4. Chemical indicator evaluation

Fig. 10 shows the observed and simulated surface indicators of O_3/NO_x , DSN, GR, and AdjGR at various sites. The results are based on 6-year seasonal average and annual average. The concentrations of NO_x used for the evaluation are the sum of concentrations of NO and NO_2 at all these sites except South Korea and EANET, where the concentrations of NO_x only include NO_2 due to the unavailable NO observations at those sites. As shown in Fig. 10, the O_3/NO_x indicator is largely overpredicted by 1–2 orders of magnitudes over Hong Kong and by factors of 3–10 over Taiwan, 7–9 over Japan, and 5–6 over South Korea during all seasons, mainly due to large

underpredictions of NO_x and overpredictions of O_3 over these sites. Similar performance of the O_3/NO_x indicator is also found at the EANET sites, with NMBs of 161.2% (winter) to 241.1% (fall), which are also mainly due to underpredictions of NO_2 . Uncertainties exist in the threshold value of O_3/NO_x in determining the VOC- or NO_x -limited O_3 chemistry. For example, Tonnesen and Dennis (2000a) used $\text{O}_3/\text{NO}_x < 15$ and Y. Zhang et al. (2009) suggested $\text{O}_3/\text{NO}_x < 60$ to indicate VOC-limited O_3 chemistry. Despite large differences in the observed and simulated O_3/NO_x values, they both are smaller than 15 at most sites (except for the simulated O_3/NO_x values in Japan and at the EANET sites that are higher than 15 but lower than 60), indicating a VOC-limited O_3 formation. The higher simulated values of O_3/NO_x indicate that the model underpredicts the extent of VOC-limited O_3 chemistry at those sites.

As shown in Fig. 11, the predicted surface O_3/NO_x values are less than 60 over central/eastern China, North/South Korea, and Japan in summer, indicating VOC-limited O_3 chemistry over those regions. The VOC-limited O_3 chemistry regime extends into larger areas in winter. Liu et al. (2010b) used a threshold value of 15 for surface O_3/NO_x over East Asia in 2008, and reported a dominance of NO_x -limited regime in July and VOC-limited regime in January. While the use of 15 instead of 60 as a threshold value in this work will bring a closer agreement in the simulated chemical regimes to the work of Liu et al. (2010b), the WRF-CAM5 simulations reported here tend to predict a VOC-chemistry in greater areas than Liu et al. (2010b), partly because of an unusual reduction of NO_x emissions prior to the 2008 Beijing Olympic games in China and partly because of differences in the gas-phase chemistry and model

Table 4
6-yr average performance statistics for chemical variables from the WRF-CAM5 simulations.

Variable	Dataset	6-yr average							
		Number	Mean Obs.	Mean Sim.	MB	NMB, %	NME, %	RMSE	R
CO	Hong Kong	52584	884.3	503.3	−381.0	−43.1	47.6	508.6	0.3
	Taiwan	1915	0.5	0.2	−0.2	−47.8	49.4	0.3	0.4
	Japan	8031	0.5	0.2	−0.3	−60.2	61.2	34.7	0.1
	South Korea	2435	0.5	0.2	−0.3	−51.9	57.3	0.4	0.1
Col. CO	MOPITT	955016	2.0×10^{18}	2.1×10^{18}	1.1×10^{17}	5.5	18.8	5.3×10^{17}	0.7
SO ₂	China-API	13735	106.9	59.1	−47.8	−44.7	68.4	98.4	−0.04
	Hong Kong	52579	17.7	38.8	21.2	119.9	184.5	52.6	0.04
	Taiwan	1914	4.1	2.5	−1.5	−37.9	74.2	3.8	−0.004
	Japan	15502	2.7	1.2	−1.5	−55.8	75.3	2.7	−0.01
	South Korea	3036	4.7	4.0	−0.7	−15.2	71.4	8.6	0.1
	EANET	1145	2.3	4.3	2.0	87.1	145.5	11.0	0.5
	SCIAMACHY	691310	0.2	0.3	0.1	27.0	105.3	0.5	0.4
Col. SO ₂	Hong Kong	50747	98.3	6.3	−92.0	−93.5	93.6	111.8	0.1
	Taiwan	1915	5.2	0.8	−4.4	−84.3	87.8	6.0	0.2
	Japan-NIES	15915	7.3	0.4	−6.9	−94.0	95.2	10.1	−0.02
	China-API	311	123.9	29.2	−94.7	−76.4	77.0	105.7	−0.04
NO ₂	Hong Kong	52579	63.9	32.9	−31.0	−48.5	62.5	48.6	0.3
	Taiwan	1915	14.6	7.0	−7.7	−52.3	62.8	11.4	0.02
	Japan	15908	11.4	4.3	−7.1	−62.3	73.9	10.4	−0.05
	South Korea	3108	16.3	8.8	−7.6	−46.2	62.7	12.7	0.2
	EANET	245	9.0	4.7	−4.4	−48.2	61.1	8.5	0.5
	SCIAMACHY	838094	2.7×10^{15}	2.5×10^{15}	$−1.9 \times 10^{14}$	−6.9	54.4	3.9×10^{15}	0.8
	Hong Kong	52579	36.4	60.5	24.1	66.3	99.4	48.3	0.5
O ₃	Taiwan	1915	30.1	35.9	5.8	19.1	29.5	10.7	0.3
	Japan	14267	31.6	34.9	3.3	10.5	24.2	9.6	0.4
	South Korea	3108	26.1	34.5	8.4	32.0	44.7	14.3	0.4
	EANET	775	37.6	37.6	0.01	0.01	26.9	12.8	0.4
	OMI/MSL	800946	30.5	33.5	3.0	10.0	16.4	6.3	0.7
	SCIAMACHY	742671	5.5×10^{15}	6.6×10^{15}	1.1×10^{15}	19.6	52.0	3.9×10^{15}	0.6
	Hong Kong	52575	37.1	51.9	14.8	40.0	86.9	58.9	0.3
TOC	Taiwan	1631	31.2	13.3	−17.9	−57.4	58.9	22.6	0.3
	EANET	71	13.8	9.3	−4.5	−32.3	36.1	6.2	0.4
	China-API	5663	95.2	80.2	−15.1	−15.8	56.5	69.7	0.1
	Hong Kong	52579	54.9	53.9	−1.0	−1.8	66.9	59.7	0.3
	Taiwan	1918	55.4	17.5	−38.0	−68.5	68.7	44.2	0.3
	Japan	16177	22.1	12.7	−9.4	−42.5	53.8	14.6	−0.03
	South Korea	3165	47.0	26.0	−21.0	−44.6	52.7	29.1	0.3
Col. HCHO/Col. NO ₂	EANET	785	33.7	18.8	−14.9	−44.1	46.4	20.8	0.7
	SCIAMACHY	664603	6.3	9.6	3.3	51.7	111.0	24.9	0.2

The units are in ppm for surface CO at all sites, ppb for all gases other than CO at Taiwan, Japan, and South Korean, and $\mu\text{g m}^{-3}$ for SO₂ and NO₂ from Mainland China –API, $\mu\text{g m}^{-3}$ for concentrations of all gases in Hong Kong; and $\mu\text{g m}^{-3}$ for PM_{2.5} and PM₁₀ at all sites. The units are in molecules cm^{-2} for column CO, NO₂, and HCHO, and DU for column SO₂ and TOC.

systems used. Surface ratio of HCHO and NO₂ (HCHO/NO₂) has been used as an indicator for O₃ photochemistry, with values of <1 and ≥ 1 indicating VOC- and NO_x-limited O₃ regimes, respectively (Tonnesen and Dennis, 2000a; Y. Zhang et al., 2009). The predicted HCHO/NO₂ is <1 (VOCs-limited) over North China Plain, North/South Korea, and southwestern Japan in summer, which also extends to larger areas such as central/eastern China and Japan in winter.

Column HCHO/NO₂ has been used as a photochemical indicator for O₃ chemistry (e.g., Martin et al., 2004; Campbell et al., 2015). Compared to satellite observations, the ratio of column HCHO/NO₂ indicator is largely overpredicted, with an NMB of 51.7%. The column HCHO/NO₂ indicator has a strong seasonal variability, with the best agreement with observations in spring (with an NMB of −3.9%) and the worst in fall (with an NMB of 167.4%). Y. Zhang et al. (2009) suggested that the HCHO/NO₂ values of ≥ 1 indicate a NO_x-limited O₃ chemistry. As shown in Fig. 8, during summer, while the observed column HCHO/NO₂ values indicate a NO_x-limited O₃ chemistry over most of the domain except for North China Plain, North Korea, and northern Japan where O₃ chemistry is VOC-limited, the simulated column HCHO/NO₂ values indicate a NO_x-limited O₃ chemistry over nearly the entire domain except for several big cities such as the larger Beijing and Shanghai areas.

Much higher simulated values of column HCHO/NO₂ than observations indicate that the model overpredicts the extent of NO_x-limited chemistry over most of the domain in summer. Such overpredictions are mainly due to the overprediction of HCHO column over eastern China. As shown in Fig. 9, during winter, the model reproduces well the VOC-limited chemistry (HCHO/NO₂ < 1) over North China Plain, South Korea, and Japan. While both simulated and observed column HCHO/NO₂ values indicate a NO_x-limited O₃ chemistry in remaining areas, the model underpredicts the extent of the NO_x-limited chemistry over the ocean and western China in winter. Such underpredictions are mainly due to the underprediction of HCHO column over the ocean and western China. Overall, the O₃ chemistry regimes simulated by WRF-CAM5 in this work for both summer and winter are consistent with those simulated by Liu et al. (2010b) using a different regional model (e.g., MM5/CMAQ). These results indicate that NO_x emissions control should be applied throughout the domain areas for both summer and winter, and VOCs emissions control should be applied over North China Plain, North/South Korea, and Japan in winter.

PM indicators can only be evaluated at limited sites because of limited observations. Due to unavailable observations for major gases (e.g., NH₃ and HNO₃) at the Miyun and THU sites, only DSN is evaluated at these sites. The results are based on 6-year seasonal

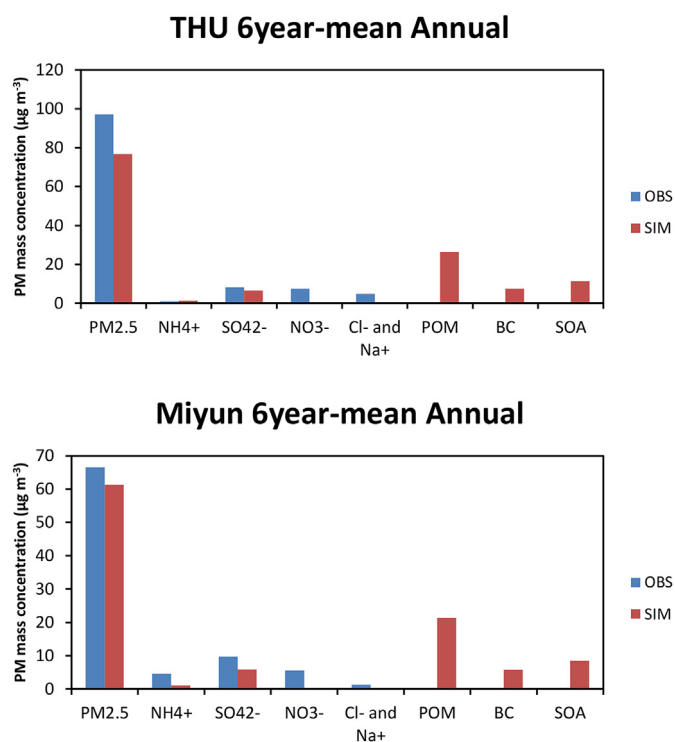


Fig. 7. 6-yr average observed and simulated concentrations of PM_{2.5} at Tsinghua (THU) and Miyun sites in Beijing, China. Note that the observations of POM, BC, and SOA are not available.

average and annual average. In WRF-CAM5 MAM3, sulfate is assumed to be present in the form of ammonium bisulfate (i.e., NH_4HSO_4). The molar ratio of NH_4 and SO_4 is always equal to 1. Also, NO_3^- is not simulated in WRF-CAM5 MAM3. Therefore, the predicted DSN is always equal to 1. At the Miyun site, the observed DSN is 1.64, and the NMB of DSN is -39.1% . At the THU site, the observed DSN is 1.59, and the NMB of DSN is -37.2% . While most studies use a threshold value of 2 to indicate a full neutralization of NH_3 to form $(\text{NH}_4)_2\text{SO}_4$, Y. Zhang et al. (2009) suggested a value of 1.5, with values < 1.5 indicating insufficiently neutralized and no NH_4NO_3 formation. The observed DSN values at both Miyun and THU are less than 2 but slightly larger than 1.5, indicating that SO_4^{2-} at those sites is fully neutralized and NH_4NO_3 can be formed to neutralize free NH_3 . In this case, the response of PM concentrations to changes in total sulfate is nonlinear (Ansari and Pandis, 1998). For comparison, the simulated DSN of 1 indicates that SO_4^{2-} at those sites is insufficiently neutralized and no NH_4NO_3 can be formed, which is inconsistent with observations. This inconsistency is because WRF-CAM5 MAM3 does not simulate NO_3^- and assumes SO_4^{2-} is neutralized by NH_4^+ as NH_4HSO_4 . While simulated DSN values agree well with observations at the EANET sites, the GR and AdjGR indicators are largely overpredicted at the EANET sites by factors of 2–3 for all seasons, with NMBs of 184.0% (spring) to 548.3% (summer) and 57.1% (fall) to 240.4% (summer), respectively. The large overpredictions of GR and AdjGR indicators are mainly due to the missing treatments for gas-particle partitioning between HNO_3 and NO_3^- and NH_3 and NH_4^+ in MAM3. At the EANET sites, the observed and simulated DSN are less than 1.5 and the observed and simulated GR and AdjGR values are greater than 1, indicating NH_3 -rich condition under which sufficient NH_3 is available to neutralize SO_4^{2-} and NO_3^- . The PM formation regimes indicated by observed DSN and GR/AdjGR are consistent at EANET where both indicators can be calculated based on observations. Fig. 11 shows the spatial

distribution of simulated indicators for O_3 chemistry (O_3/NO_x and HCHO/NO_2) and PM formation (GR and AdjGR) for summer and winter based on 6-year average. The predicted GR and AdjGR are larger than 1 over eastern China, South Korea, and Japan in both summer and winter with much larger values in summer, indicating a NH_3 -rich regime with potential NH_4NO_3 formation over those areas. Under the NH_3 -rich regime, inorganic PM formation is sensitive to total sulfate, total ammonia, and total nitrate, indicating a need to control all gaseous precursors including SO_2 , NH_3 , and NO_x . However, the model does not simulate NH_4^+ and NO_3^- , leading to the inaccurate predictions of NH_3 , HNO_3 , and SO_4^{2-} , which may affect not only predicted PM concentrations but also GR and AdjGR values.

4. Conclusions and recommendations

In this work, multi-year simulations of WRF-CAM5 are conducted and evaluated comprehensively against observations from surface networks, satellites, and aircraft. The results show that meteorological variables (e.g., T2, Q2, WS10, and precipitation) and some cloud variables (e.g., CF and PWV) are overall well predicted (with NMBs within $\pm 14.0\%$), whereas CCN5, LWP, and COT are moderately underpredicted, with NMBs of -53.5% to -35.8% , indicating possible uncertainties in the treatments of cloud dynamics and thermodynamics, the ice microphysics, and aerosol-cloud interactions. CDNC is also underpredicted, with an NMB of -18.5% , indicating potential uncertainties in the aerosol activation parameterization. IWP is largely underpredicted, with an NMB of -96.1% , suggesting some model uncertainties in the ice nucleation parameterization. Due to the underpredictions of cloud variables, SWD is overpredicted with an NMB of 11.8% and SWCF is underpredicted with an NMB of -17.4% .

The 6-year averaged surface concentrations of CO, SO_2 , NO_x , PM_{2.5}, and PM₁₀ are moderately underpredicted over most regions, which are mainly due to uncertainties in the emissions of CO, SO_2 , and NO_x , and PM. The overpredictions of 6-year averaged surface concentrations of SO_2 and PM_{2.5} over Hong Kong are likely due to overestimations in the SO_2 emissions as well as inaccurate predictions of CF. Surface O_3 mixing ratios are overpredicted at all network sites with NMBs of 10.5%–66.3%, which is likely due in part to insufficient O_3 titration resulted from underpredictions of NO mixing ratios. The CO column concentration is well predicted, with an NMB of 5.5%, despite an underprediction in surface CO mixing ratio, indicating the uncertainties in the model representation of vertical transport as well as vertical distribution of CO emissions (Y. Zhang et al., 2016a). The SO_2 column concentration is moderately overpredicted, with an NMB of 27.0%, despite an underprediction in surface SO_2 mixing ratio over most regions, indicating uncertainties in the total SO_2 emissions, their vertical distribution, and the model representation of vertical transport. The NO_2 column concentration and TOC are well predicted, whereas the HCHO column concentration is moderately overpredicted, with an NMB of 19.6%, indicating the uncertainties in the emissions (e.g., HCHO and isoprene) and chemical reactions for HCHO production and removal.

Based on the surface O_3/NO_x indicators calculated over Hong Kong, Taiwan, Japan, South Korea, and the EANET sites, the O_3 chemistry at those sites is VOC-limited. While the simulated O_3 chemistry regimes are generally consistent with the observations, the model tends to underpredict the extent of VOC-limited O_3 chemistry (i.e., overpredicts the extent of NO_x -limited O_3 chemistry) at those sites. Based on the column HCHO/ NO_2 indicators calculated over the whole domain, WRF-CAM5 predicts a NO_x -limited chemistry over nearly the whole domain except for several big cities in summer and over most of the domain except for North China Plain, North/South Korea, and Japan and in winter. While the

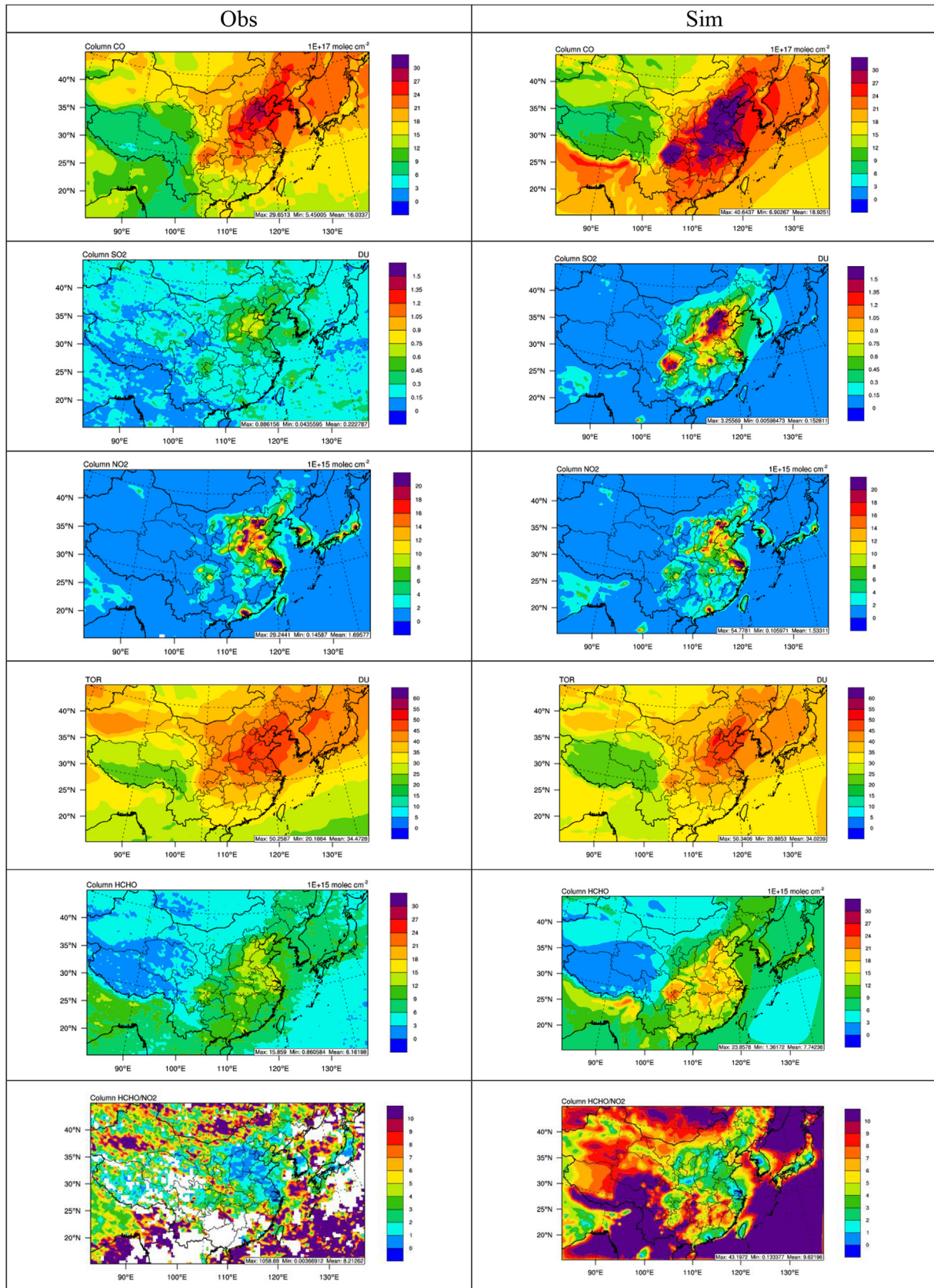


Fig. 8. Comparison of simulated 6-year average column concentrations with satellite retrievals in summer.

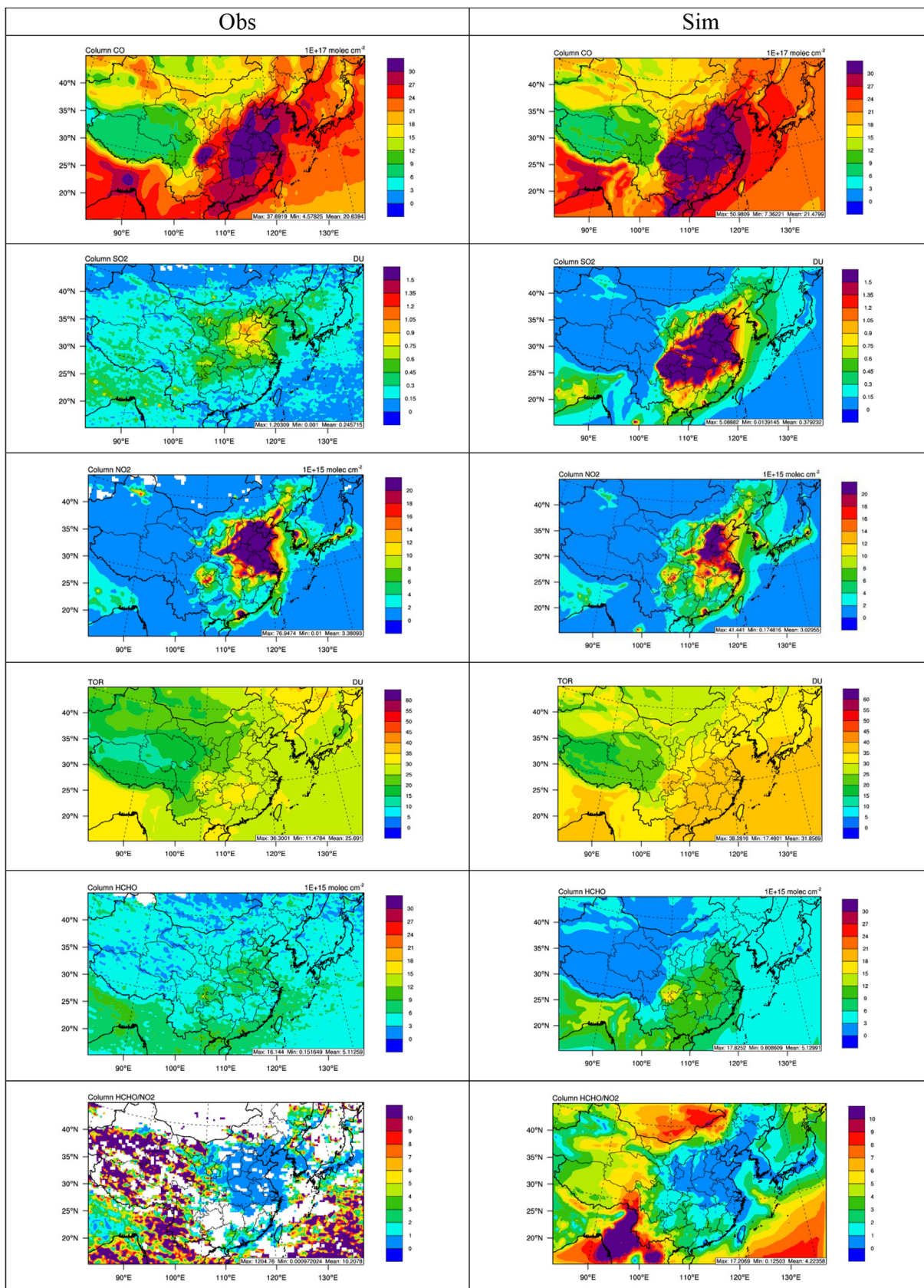


Fig. 9. Comparison of simulated 6-year average column concentrations with those from satellite retrievals in winter.

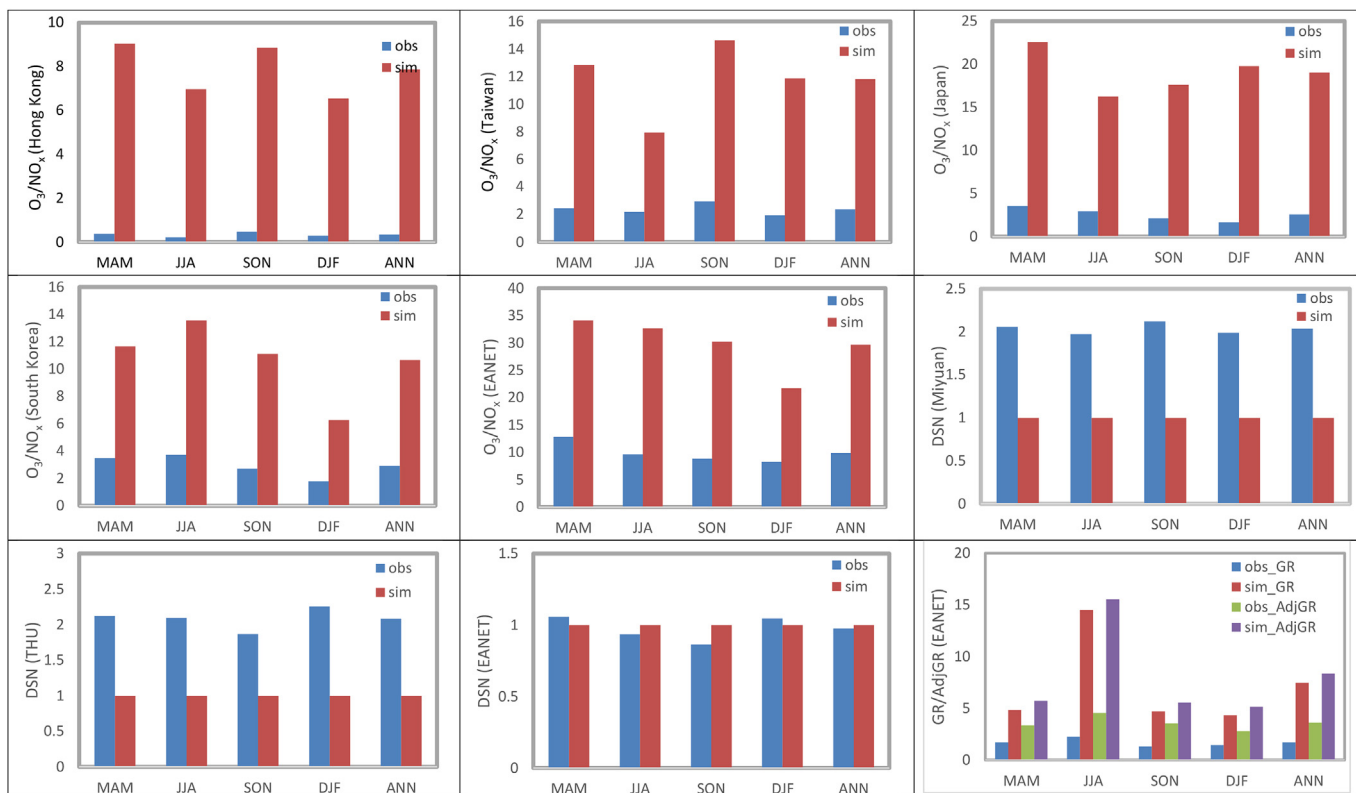


Fig. 10. Comparison of observed and simulated O_3 and PM indicators over various sites for 6-year average March–April–May (MAM), June–July–August (JJA), September–October–November (SON), December–January–February (DJF), and annual average (ANN).

simulated O_3 chemistry regimes are consistent with observations, the model tends to overpredict the extent of NO_x -limited chemistry over most of the domain in summer but underpredicts it over the ocean and western China in winter.

The O_3 chemistry regime calculations using surface values of O_3/NO_x and both surface and column values of $HCHO/NO_2$ indicate that while NO_x emissions should be controlled throughout the year, VOCs emissions should be controlled in summer in big cities and in winter over North China Plain, North/South Korea, and Japan. While the observed DSN values at both Miyun and THU sites indicate a sulfate-poor regime and potential formation of NH_4NO_3 , the model fails to reproduce the observed PM formation regime, because WRF-CAM5 MAM3 does not simulate NO_3^- and assumes SO_4^{2-} is neutralized by NH_4^+ as NH_4HSO_4 . While the observed and simulated GR and AdjGR values both indicate sulfate-poor regime at the EANET sites, the model overpredicts the GR and AdjGR indicators due to the missing treatments for gas-particle partitioning for total NH_3 and nitrate in MAM3. Inaccurate predictions of PM indicators (i.e., DSN, GR, and AdjGR) indicate that additional model improvements are needed to reduce model uncertainties in predicting gas-particle partitioning. The spatial distributions of GR and AdjGR indicate a NH_3 -rich regime over most of the domain, where inorganic PM formation is sensitive to the total sulfate, total ammonia, and total nitrate. Those results indicate a need to collectively control all gaseous precursors including SO_2 , NH_3 , and NO_x throughout the year in order to reduce inorganic PM formation.

Despite some large biases due to uncertainties in the emissions and some model treatments such as missing aerosol species and vertical transport, the model can in general reproduce meteorology, chemistry, and climate well. The model's skill is overall consistent with or outperforms most other regional models applied to East

Asia previously. The model configuration of WRF-CAM5 in this work is thus deemed to be suitable for long term regional climate simulations.

There are several areas of improvement for WRF-CAM5 and its application. Uncertainties in the model inputs such as emissions should be further reduced in the future. Uncertainties in aerosol and cloud treatments in WRF-CAM5 contribute the most to the model biases so they should be reduced in the future. For example, the current version of WRF-CAM5 does not simulate nitrate, which is an important species for aerosol components in some regions. WRF-CAM5 does not simulate aerosol thermodynamics, which is an important process for aerosol mass concentrations calculation. Explicit treatments of major aerosol species and their physical and chemical processes should be included in the future to improve model performance for aerosol species. The simulations of WRF-CAM with the default heterogeneous ice nucleation scheme of Meyers et al. (1992) (M92) show large uncertainties in ice nucleation processes (e.g., large underpredictions of IWP), which are important to the formation and properties of cirrus and mixed-phase clouds. While Y. Zhang et al. (2015b) showed a high sensitivity of the model predictions to the use of M92 and the more advanced heterogeneous ice nucleation scheme of Niemand et al. (2012) (N12), large biases in IWP and other cloud variables remain with both M92 and N12. More advanced ice nucleation schemes should be implemented into the model to improve the model performance in simulating the formation of ice crystals and their interactions with aerosol and climate in the future. Finally, a finer grid resolution should be used, whenever possible, to resolve fine-scale features such as complex coastline and terrain in the Korean Peninsula and Japan where larger biases in surface climate are noted in our simulations. The inclusion of physical

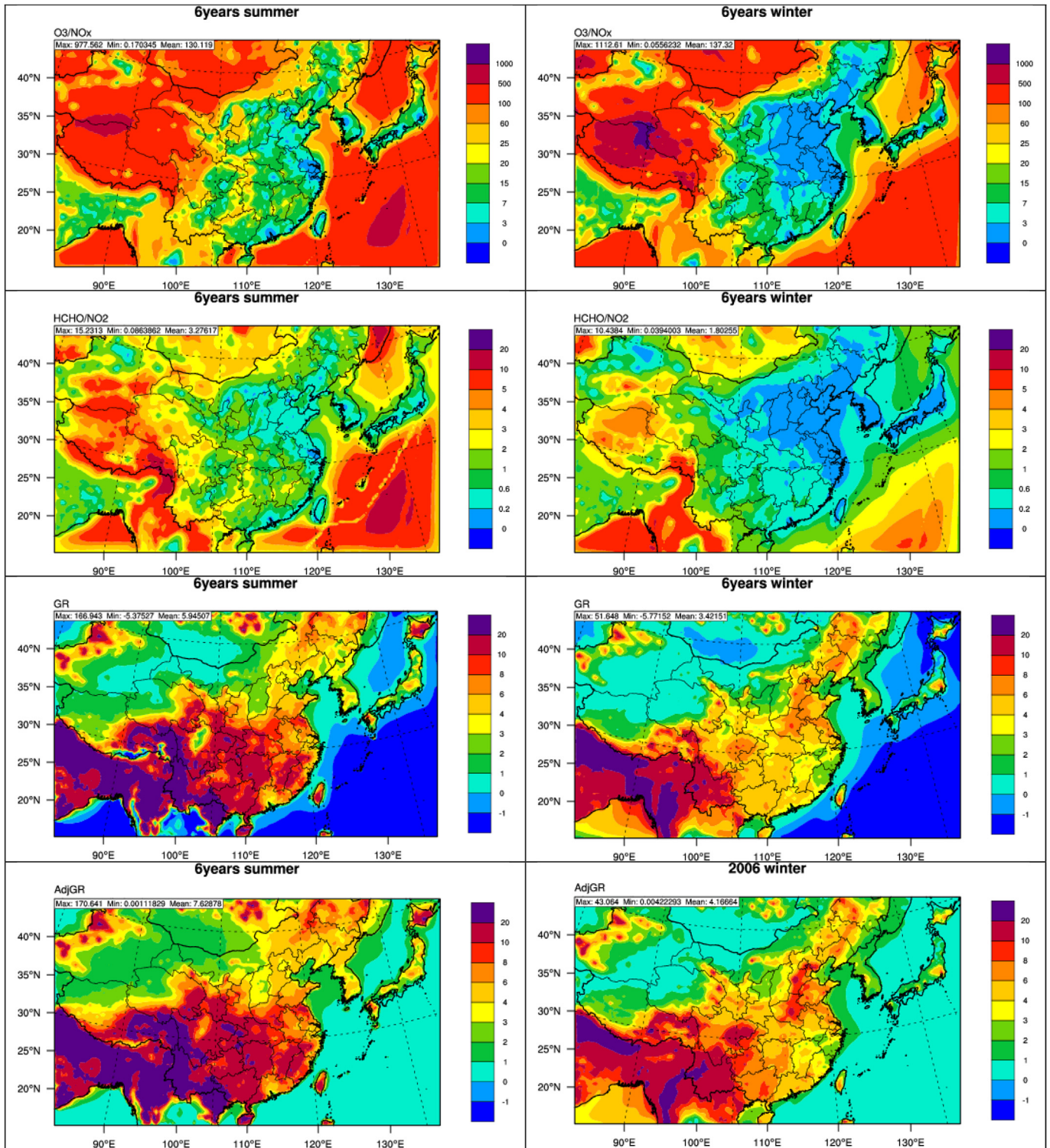


Fig. 11. Spatial distribution of simulated surface O₃/NO_x indicator, HCHO/NO₂ indicator, GR, and AdjGR indicators for summer (left column) and winter (right column).

parameterizations with scale-awareness in the future model improvement could help improve the meteorological predictions. Nested simulations at 12-km over eastern China and 4-km over Beijing and Shanghai areas driven with ICs and BCs derived from the outputs of WRF-CAM5 at 36-km in this work are ongoing and will be reported in the future.

Acknowledgments

This research was supported by the U.S. Department of Energy Office of Science Biological and Environmental Research as part of the Global and Regional Climate Modeling programs (DE-SC0006695 at North Carolina State University and KP1703000 at Pacific Northwest National Laboratory) and China's National Basic Research Program (2010CB951803 at Tsinghua University). Observations in mainland China, Taiwan, Hong Kong, Japan, and South Korea as well as satellite data were downloaded from their respective websites. The authors acknowledge high-performance computing support from Kraken and Stampede, provided as an Extreme Science and Engineering Discovery Environment (XSEDE) digital service by the Texas Advanced Computing Center (TACC) (<http://www.tacc.utexas.edu>), which is supported by National Science Foundation grant number ACI-1053575., and the National Energy Research Scientific Computing Center (NERSC), which is supported by the Office of Science of the U.S. Department of Energy under Contract No. DE-AC02-05CH11231. The Pacific Northwest National Laboratory is operated by Battelle for the U.S. Department of Energy under Contract DE-AC05-76RLO1830.

The data used to generate results presented in this paper will be available free of charge upon request, please contact Yang Zhang at yhzhang9@ncsu.edu.

Appendix A. Supplementary data

Supplementary data related to this article can be found at <http://dx.doi.org/10.1016/j.atmosenv.2017.06.015>.

References

- Abdul-Razzak, H., Ghan, S.J., 2000. A parameterization of aerosol activation 2. Multiple aerosol types. *J. Geophys. Res.* 105 (D5), 6837–6844. <http://dx.doi.org/10.1029/1999JD901161>.
- Ansari, A.S., Pandis, S.N., 1998. Response of inorganic PM to precursor concentrations. *Environ. Sci. Technol.* 32, 2706–2714.
- Barth, M.C., Rasch, P.J., Kiehl, J.T., Benkovitz, C.M., Schwartz, S.E., 2000. Sulfur chemistry in the national center for atmospheric research community climate model: description, evaluation, features and sensitivity to aqueous chemistry. *J. Geophys. Res.* 105, 1387–1415.
- Bennartz, R., 2007. Global assessment of marine boundary layer cloud droplet number concentration from satellite. *J. Geophys. Res.* 112, D02201. <http://dx.doi.org/10.1029/2006JD007547>.
- Binkowski, F.S., Roselle, S.J., 2003. Models-3 community multiscale air quality (CMAQ) model aerosol component, 1, model description. *J. Geophys. Res.* 108 (D6), 4183. <http://dx.doi.org/10.1029/2001JD001409>.
- Bretherton, C.S., Park, S., 2009. A new moist turbulence parameterization in the Community Atmosphere Model. *J. Clim.* 22, 3422–3448.
- Byun, D., Schere, K.L., 2006. Review of the governing equations, computational algorithms, and other components of the Models-3 Community Multiscale Air Quality (CMAQ) modeling system. *Appl. Mech. Rev.* 59, 51–77.
- Cai, C.-J., Zhang, X., Wang, K., Zhang, Y., Wang, L.-T., Zhang, Q., Duan, F.-K., He, K.-B., Yu, S.-C., 2015. Incorporation of new particle formation and early growth treatments into WRF/Chem and its application over East Asia: model improvement, evaluation, and the Nucleation-Aerosol-Cloud-Meteorology interactions. *Atmos. Environ.* <http://dx.doi.org/10.1016/j.atmosenv.2015.05.046>.
- Campbell, P., Zhang, Y., Yahya, K., Wang, K., Hogrefe, C., Pouliot, G., Knote, C., Hodzic, A., Jose, R.S., Perez, J.L., Guerrero, P.J., Baro, R., Makar, P., 2015. A multi-model assessment for the 2006 and 2010 simulations under the Air Quality Model Evaluation International Initiative (AQMEII) phase 2 over North America: Part I. Indicators of the sensitivity of O₃ and PM_{2.5} formation regimes. *Atmos. Environ.* 115, 569–586.
- Chen, F., Duhia, J., 2001. Coupling an advanced land surface-hydrology model with the Penn State-NCAR MM5 modeling system. Part I: model implementation and sensitivity. *Mon. Weather Rev.* 129, 569–585.
- Chen, Y., Zhang, Y., Fan, J.-W., Leung, L.-Y.R., Zhang, Q., He, K.-B., 2015. Application of an online-coupled regional climate model, WRF-CAM5, over East Asia for examination of ice nucleation schemes: Part I. Comprehensive model evaluation and trend analysis for 2006 and 2011. *Climate* 3, 627–667.
- Chu, D.A., Remer, L.A., Kaufman, Y.J., Schmid, B., Redemann, J., Knobelspiesse, K., Chern, J.-D., Livingston, J., Russell, P.B., Xiong, X., Ridgeway, W., 2005. Evaluation of aerosol properties over ocean from moderate resolution imaging spectroradiometer (MODIS) during ACE-Asia. *J. Geophys. Res.* 110, D07308. <http://dx.doi.org/10.1029/2004JD005208>.
- De Smedt, I., Müller, J.-F., Stavrou, T., van der, R.J., Eskes, A.H.J., van Roozendaal, M., 2008. Twelve years of global observations of formaldehyde in the troposphere using GOME and SCIAMACHY sensors. *Atmos. Chem. Phys.* 2008 (8), 4947–4963.
- Ek, M.B., Mitchell, K.B., Lin, Y., Rogers, B., Grunmann, P., Koren, V., Gayno, G., Tarpley, J.D., 2003. Implementation of NOAA land surface model advances in the National Centers for Environmental Prediction operational mesoscale eta model. *J. Geophys. Res.* 108 (D22), 8851. <http://dx.doi.org/10.1029/2002JD003296>.
- Forster, P., Ramaswamy, V., Artaxo, P., Bernsten, T., Betts, R., Fahey, D.W., Haywood, J., Lean, J., Lowe, D.C., Myhre, G., Nganga, J., Prinn, R., Raga, G., Schulz, M., Van Dorland, R., 2007. Changes in atmospheric constituents and in radiative forcing. In: Solomon, S. (Ed.), *Climate Change 2007: The Physical Science Basis*. Cambridge University Press, Cambridge, United Kingdom and New York, NY, USA.
- Fountoukis, C., Nenes, A., 2007. ISORROPIA II: a computationally efficient thermodynamic equilibrium model for K⁺-Ca²⁺-Mg²⁺-NH₄⁺-Na⁺-SO₄²⁻-NO₃⁻-Cl⁻-H₂O aerosols. *Atmos. Chem. Phys.* 7, 4639–4659. <http://dx.doi.org/10.5194/acp-7-4639-2007>.
- Gilmore, M.S., Straka, J.M., Rasmussen, E.N., 2004. Precipitation uncertainty due to variations in precipitation particle parameters within a simple microphysics scheme. *Mon. Wea. Rev.* 132, 2610–2627. <http://dx.doi.org/10.1175/MWR2810.1>.
- Giorgi, F., Bi, X., Qian, Y., 2002. Direct radiative forcing and regional climatic effects of anthropogenic aerosols over East Asia: a regional coupled climate-chemistry/aerosol model study. *J. Geophys. Res.* 107 (D20), 4439. <http://dx.doi.org/10.1029/2001JD001066>.
- Giorgi, F., Bi, X.Q., Qian, Y., 2003. Indirect vs. direct effects of anthropogenic sulfate on the climate of East Asia as simulated with a regional coupled climate-chemistry/aerosol model. *Clim. Change* 58, 345–376.
- Gong, S.L., Barrie, L.A., Lazare, M., 2002. Canadian Aerosol Module (CAM): a size-segregated simulation of atmospheric aerosol processes for climate and air quality models: 2. Global sea-salt aerosol and its budgets. *J. Geophys. Res.* 107 (D24), 4779. <http://dx.doi.org/10.1029/2001JD002004>.
- Grell, G.A., Peckham, S.E., Schmitz, R., McKeen, S.A., Frost, G., Skamarock, W.C., Eder, B., 2005. Fully coupled “online” chemistry within the WRF model. *Atmos. Environ.* 39, 6957–6975.
- Guenther, A.B., Karl, T., Harley, P., Wiedinmyer, C., Palmer, P.I., Geron, C., 2006. Estimates of global terrestrial isoprene emissions using MEGAN (a model of emissions of gases and aerosols from nature). *Atmos. Chem. Phys.* 6, 3181–3210.
- Han, Z., 2010. Direct radiative effect of aerosols over East Asia with a regional coupled climate/chemistry model. *Meteorol. Z.* 19, 287–298.
- Han, Z.W., Li, J.-W., Xia, X.-A., Zhang, R.-J., 2012. Investigation of direct radiative effects of aerosols in dust storm season over East Asia with an online coupled regional climate-chemistry-aerosol model. *Atmos. Environ.* 54, 688–699.
- Han, Z.W., Li, J.-W., Guo, W.-D., Xiong, Z., Zhang, W., 2013. A study of dust radiative feedback on dust cycle and meteorology over East Asia by a coupled regional climate-chemistry-aerosol model. *Atmos. Environ.* 68, 54–63.
- Hao, N., Valks, P., Loyola, D., Cheng, V.F., Zimmer, W., 2011. Space-based measurements of air quality during the World Expo 2010 in Shanghai. *Environ. Res. Lett.* 6 <http://dx.doi.org/10.1088/1748-9326/6/4/044004>.
- He, J., Zhang, Y., 2014. Improvement and further development in CESM/CAM5: gas-phase chemistry and inorganic aerosol treatments. *Atmos. Chem. Phys.* 14, 9171–9200. <http://dx.doi.org/10.5194/acp-14-9171-2014>.
- He, K.-B., 2012. Multi-resolution emission inventory for China (MEIC): model framework and 1990–2010 anthropogenic emissions. In: *Proceedings of the International Global Atmospheric Chemistry Conference*. Beijing, China, September 2012.
- He, J., Zhang, Y., Glotfelty, T., He, R., Bennartz, R., Rausch, J., Sartelet, K., 2015. Decadal simulation and comprehensive evaluation of CESM/CAM5. 1 with advanced chemistry, aerosol microphysics, and aerosol-cloud interactions. *J. Adv. Model. Earth Syst.* 7, 110–141. <http://dx.doi.org/10.1002/2014MS000360>.
- Hong, C.-P., Zhang, Q., He, K.-B., Guan, D.-B., Li, M., Liu, F., Zheng, B., 2017. Variations of China's emission estimates: response to uncertainties in energy statistics. *Atmos. Chem. Phys.* 17, 1227–1239.
- Huo, H., Zhang, Q., He, K.-B., Wang, Q.-D., Yao, Z.-L., Streets, D.G., 2009. High-resolution vehicular emission inventory using a link-based method: a case study of light-duty vehicles in Beijing. *Environ. Sci. Technol.* 43 (7), 2394–2399. <http://dx.doi.org/10.1021/es802757a>, 2009.
- Iacono, M.J., Delamere, J.S., Mlawer, E.J., Shephard, M.W., Clough, S.A., Collins, W.D., 2008. Radiative forcing by long-lived greenhouse gases: calculations with the AER radiative transfer models. *J. Geophys. Res.* 113, D13103. <http://dx.doi.org/10.1029/2008JD009944>.
- Jacobson, M.Z., 2001a. GATOC-GCMM: a global-through urban-scale air pollution and weather forecast model 1. Model design and treatment of subgrid soil, vegetation, roads, rooftops, water, sea, ice, and snow. *J. Geophys. Res.* 106, 5385–5401.

- Jacobson, M.Z., 2001b. GATOC-GCMM: 2. A study of day- and nighttime ozone layers aloft, ozone in national parks, and weather during the SARMAP Field Campaign. *J. Geophys. Res.* 106, 5403–5420.
- Lacis, A.A., Wuebbles, D.J., Logan, J.A., 1990. Radiative forcing of climate by changes in the vertical distribution of ozone. *J. Geophys. Res.* 95, 9971–9981.
- Lamarque, J.F., Emmons, L.K., Hess, P.G., Kinnison, D.E., Tilmes, S., Vitt, F., Heald, C.L., Holland, E.A., Lauritzen, P.H., Neu, J., Orlando, J.J., Rasch, P.J., Tyndall, G.K., 2012. CAM-chem: description and evaluation of interactive atmospheric chemistry in CESM. *Geosci. Model Dev.* 5, 369–411. <http://dx.doi.org/10.5194/gmd-5-369-2012>.
- Lee, C., Martin, R.V., van Donkelaar, A., O'Byrne, G., Krotkov, N., Richter, A., Huey, L.G., Holloway, J.S., 2009. Retrieval of vertical columns of sulfur dioxide from SCIAMACHY and OMI: air mass factor algorithm development, validation, and error analysis. *J. Geophys. Res.* 114, D22303. <http://dx.doi.org/10.1029/2009JD012123>.
- Lim, K.-S., Fan, J.-W., Leung, L.R., Ma, P.-L., Singh, B., Zhao, C., Zhang, Y., Zhang, G., Song, X.-L., 2014. Investigation of aerosol indirect effects using a cumulus microphysics parameterization with an A Regional climate model. *J. Geophys. Res.* 116, D02204. <http://dx.doi.org/10.1002/2013JD020958>.
- Lin, M., Holloway, T., Carmichael, G.R., Fiore, A.M., 2010. Quantifying pollution inflow and outflow over East Asia in spring with regional and global models. *Atmos. Chem. Phys.* 10, 4221–4239. <http://dx.doi.org/10.5194/acp-10-4221-2010>.
- Liu, X., Easter, R.C., Ghan, S.J., Zaveri, R., Rasch, P., Shi, X., Lamarque, J.-F., Gettelman, A., Morrison, H., Vitt, F., Conley, A., Park, S., Neale, R., Hannay, C., Ekman, A.M.L., Hess, P., Mahowald, N., Collins, W., Iacono, M.J., Bretherton, C.S., Flanner, M.G., Mitchell, D., 2012. Toward a minimal representation of aerosols in climate models: description and evaluation in the Community Atmosphere Model CAM5. *Geosci. Model Dev.* 5, 709–739. <http://dx.doi.org/10.5194/gmd-5-709-2012>.
- Liu, X.H., Zhang, Y., Cheng, S.H., Xing, J., Zhang, Q., Streets, D.G., Jang, C.J., Wang, W.X., Hao, J.M., 2010a. Understanding of regional air pollution over China using CMAQ, Part I. Performance evaluation and seasonal variation. *Atmos. Environ.* 44, 2415–2426.
- Liu, X.H., Zhang, Y., Xing, J., Zhang, Q., Wang, K., Streets, D.G., Jang, C.J., Wang, W.X., Hao, J.M., 2010b. Understanding of regional air pollution over China using CMAQ, part II. Process analysis and sensitivity of ozone and particulate matter to precursor emissions. *Atmos. Environ.* 44, 3719–3727.
- Liu, X.-Y., Zhang, Y., Zhang, Q., He, K.-B., 2016. Application of online-coupled WRF/Chem-MADRID in East Asia: model evaluation and climatic effects of anthropogenic aerosols. *Atmos. Environ.* 124, 321–336.
- Lu, Z., Streets, D.G., Zhang, Q., Wang, S., Carmichael, G.R., Cheng, Y.F., Wei, C., Chin, M., Diehl, T., Tan, Q., 2010. Sulfur dioxide emissions in China and sulfur trends in East Asia since 2000. *Atmos. Chem. Phys.* 10, 6311–6331. <http://dx.doi.org/10.5194/acp-10-6311-2010>.
- Ma, P.-L., Rasch, P.J., Fast, J.D., Easter, R.C., Gustafson Jr., W.I., Liu, X., Ghan, S.J., Singh, B., 2013. Assessing the CAM5 physics suite in the WRF-Chem model: implementation, evaluation, and resolution sensitivity. *Geosci. Model Dev.* 7, 755–778.
- Madronich, S., 1987. Photodissociation in the atmosphere: 1. Actinic flux and the effect of ground reflections and clouds. *J. Geophys. Res.* 92, 9740–9752.
- Martin, R.V., Fiore, A.M., Donkelaar, A.V., 2004. Space-based diagnosis of surface ozone sensitivity to anthropogenic emissions. *Geophys. Res. Lett.* 31, L06120. <http://dx.doi.org/10.1029/2004GL019416>.
- McFarquhar, G.M., Zhang, H., Heymsfield, G., Hood, R., Dudhia, J., Halverson, J.B., Marks Jr., F., 2006. Factors affecting the evolution of Hurricane Erin (2001) and the distributions of hydrometeors: role of microphysical processes. *J. Atmos. Sci.* 63, 127–150. <http://dx.doi.org/10.1175/JAS3590.1>.
- Meyers, M.P., DeMott, P.J., Cotton, W.R., 1992. New primary ice-nucleation parameterizations in an explicit cloud model. *J. Appl. Meteorol.* 31, 708–721. [http://dx.doi.org/10.1175/1520-0450\(1992\)031<0708:NPINPI>2.0.CO;2](http://dx.doi.org/10.1175/1520-0450(1992)031<0708:NPINPI>2.0.CO;2).
- Mlawer, E.J., Taubman, S.J., Brown, P.D., Iacono, M.J., Clough, S.A., 1997. Radiative transfer for inhomogeneous atmospheres: RRTM, a validated correlated-k model for the longwave. *J. Geophys. Res.* 102 (D14), 16,663–16,682. <http://dx.doi.org/10.1029/97JD00237>.
- Morrison, H., Gettelman, A., 2008. A new two-moment bulk stratiform cloud microphysics scheme in the Community Atmosphere Model, version 3 (CAM3). Part I: description and numerical tests. *J. Clim.* 21, 3642–3659.
- Morrison, H., Grabowski, W.W., 2008. A novel approach for representing ice microphysics in models: description and tests using a kinematic framework. *J. Atmos. Sci.* 65, 1528–1548. <http://dx.doi.org/10.1175/2007JAS2491.1>.
- Niemand, M., Mohler, O., Vogel, B., Vogel, H., Hoese, C., Connolly, P., Klein, H., Bingemer, H., DeMott, P., Skrotzki, J., Leisner, T., 2012. A particle-surface-area-based parameterization of immersion freezing on desert dust particles. *J. Atmos. Sci.* 69, 3077–3092.
- Pal, J.S., Giorgi, F., Bi, X.-Q., Elguindi, N., Solmon, F., Rauscher, S.A., Gao, X.-J., Francisco, R., Zakey, A., Winter, J., Ashfaq, M., Syed, F.S., Sloan, L.C., Bell, J.L., Diffenbaugh, N.S., Karmacharya, J., Konar, A., Martinez, D., da Rocha, R.P., Steiner, A.L., 2007. Regional climate modeling for the developing World: the ICTP RegCM3 and RegCNET. *Bull. Amer. Meteor. Soc.* 88, 1395–1409. <http://dx.doi.org/10.1175/BAMS-88-9-1395>.
- Pinder, R.W., Dennis, R.L., Bhawe, P.V., 2008. Observable indicators of the sensitivity of PM_{2.5} nitrate to emission reductions: part I. Derivation of the adjusted gas ratio and applicability at regulatory-relevant time scales. *Atmos. Environ.* 42 (6), 1275–1286.
- Seethala, C., Horváth, Á., 2010. Global assessment of AMSR-E and MODIS cloud liquid water path retrievals in warm oceanic clouds. *J. Geophys. Res.* 115, D13202. <http://dx.doi.org/10.1029/2009JD012662>.
- Song, X., Zhang, G.J., 2011. Microphysics parameterization for convective clouds in a global climate model: description and single-column model tests. *J. Geophys. Res.* 116, D02201. <http://dx.doi.org/10.1029/2010JD014833>.
- Stevenson, D.S., Young, P.J., Naik, V., Lamarque, J.-F., Shindell, D.T., Voulgarakis, A., Skeie, R.B., Dalsoren, S.B., Myhre, G., Bernsten, T.K., Folberth, G.A., Rumbold, S.T., Collins, W.J., MacKenzie, I.A., Doherty, R.M., Zeng, G., van Noije, T.P.C., Strunk, A., Bergmann, D., Cameron-Smith, P., Plummer, D.A., Strode, S.A., Horowitz, L., Lee, Y.H., Szopa, S., Sudo, K., Nagashima, T., Josse, B., Cionni, I., Righi, M., Eyring, V., Conley, A., Bowman, K.W., Wild, O., Archibald, A., 2013. Tropospheric ozone changes, radiative forcing and attribution to emissions in the atmospheric chemistry and climate model intercomparison Project (ACCMIP). *Atmos. Chem. Phys.* 13, 3063–3085. <http://dx.doi.org/10.5194/acp-13-3063-2013>.
- Tilmes, S., Lamarque, J.-F., Emmons, L.K., Kinnison, D.E., Ma, P.-L., Liu, X., Ghan, S., Bardeen, C., Arnold, S., Deeter, M., Vitt, F., Ryerson, T., Elkins, J.W., Moore, F., Spackman, R., Martin, M.V., 2015. Description and evaluation of tropospheric chemistry and aerosols in the community Earth system model (CESM1.2). *Geosci. Model Dev.* 8, 1395–1426. <http://dx.doi.org/10.5194/gmd-8-1395-2015>.
- Tonnenes, G.S., Dennis, R.L., 2000a. Analysis of radical propagation efficiency to assess ozone sensitivity to hydrocarbons and NO_x: 1. Local indicators of instantaneous odd oxygen production sensitivity. *J. Geophys. Res.* 105, 9213–9225. <http://dx.doi.org/10.1029/1999JD000371>.
- Wang, K., Zhang, Y., Nenes, A., Fountoukis, C., 2012. Implementation of dust emission and chemistry into the Community Multiscale Air Quality Modeling System and initial application to an Asian dust storm episode. *Atmos. Chem. Phys.* 12, 10,209–10,237.
- Wang, L.-T., Jang, C., Zhang, Y., Wang, K., Zhang, Q., Streets, D., Fu, J., Lei, Y., Schreifels, J., He, K.-B., Hao, J.-M., Lam, Y.-F., Lin, J., Meskhidze, N., Voorhees, S., Everts, D., Phillips, S., 2010a. Assessment of air quality benefits from national air pollution control policies in China. Part I: background, emission scenarios and evaluation of meteorological predictions. *Atmos. Environ.* 44, 3442–3448.
- Wang, L.-T., Jang, C., Zhang, Y., Wang, K., Zhang, Q., Streets, D., Fu, J., Lei, Y., Schreifels, J., He, K.-B., Hao, J.-M., Lam, Y.-F., Lin, J., Meskhidze, N., Voorhees, S., Everts, D., Phillips, S., 2010b. Assessment of air quality benefits from national air pollution control policies in China. Part II: evaluation of air quality predictions and air quality benefits assessment. *Atmos. Environ.* 44 (28), 3449–3457. <http://dx.doi.org/10.1016/j.atmosenv.2010.05.051>.
- Wang, L.-L., Xin, J.-Y., Wang, Y.-S., Li, Z.-Q., Liu, G.-R., Li, J., 2007. Evaluation of the MODIS aerosol optical depth retrieval over different ecosystems in China during EAST-AIRE. *Atmos. Environ.* 41 (33), 7138–7149.
- Wang, L.-T., Zhang, Y., Wang, K., Zheng, B., Zhang, Q., 2014. Application of online Weather Research Forecasting Model with Chemistry (WRF/Chem) over the north China: sensitivity study, comparative evaluation and policy implications. *Atmos. Environ.* <http://dx.doi.org/10.1016/j.atmosenv.2014.12.052>.
- Wang, X.-Y., Liang, X.-Z., Jiang, W.-M., Tao, Z.-N., Wang, J.X.L., Liu, H.-N., Han, Z.-W., Liu, S.-Y., Zhang, Y.-Y., Grell, G.A., Peckham, S.E., 2010. WRF-Chem simulation of East Asian air quality: sensitivity to temporal and vertical emissions distributions. *Atmos. Environ.* 44, 660–669. <http://dx.doi.org/10.1016/j.atmosenv.2009.11.011>.
- Wang, T.J., Li, S., Shen, Y., Deng, J.J., Xie, M., 2010. Investigations on direct and indirect effect of nitrate on temperature and precipitation in China using a regional climate chemistry modeling system. *J. Geophys. Res.* 115, D00K26. <http://dx.doi.org/10.1029/2009JD013264>.
- Wang, T.J., Zhuang, B.L., Li, S., Liu, J., Xie, M., Yin, C.Q., Zhang, Y., Yuan, C., Zhu, J.L., Ji, L.Q., Han, Y., 2015. The interactions between anthropogenic aerosols and the East Asian summer monsoon using RegCM3. *J. Geophys. Res.* 120, 5602–5621. <http://dx.doi.org/10.1002/2014JD022877>.
- Witte, J.C., Schoeberl, M.R., Douglass, A.R., Gleason, J.F., Krotkov, N.A., Gille, J.C., Pickering, K.E., Livesey, N., 2009. Satellite observations of changes in air quality during the 2008 Beijing Olympics and Paralympics. *Geophys. Res. Lett.* 36, L17803. <http://dx.doi.org/10.1029/2009GL039236>.
- Wong, D.C., Pleim, J., Mathur, R., Binkowski, F., Otte, T., Gilliam, R., Pouliot, G., Xiu, A., Young, J.O., Kang, D., 2012. WRF-CMAQ two-way coupled system with aerosol feedback: software development and preliminary results. *Geosci. Model Dev.* 5, 299–312. <http://dx.doi.org/10.5194/gmd-5-299-2012>.
- Yahya, K., Wang, K., Campbell, P., Chen, Y., Glotfeldt, T., He, J., Pirhalla, M., Zhang, Y., 2017. Decadal application of WRF/chem for regional air quality and climate modeling over the U.S. under the representative concentration pathways scenarios. Part 1: model evaluation and impact of downscaling. *Atmos. Environ.* 152, 562–583. <http://dx.doi.org/10.1016/j.atmosenv.2016.12.029>.
- Yu, S., Eder, B., Dennis, R., Chu, S.-H., Schwartz, S., 2006. New unbiased symmetric metrics for evaluation of air quality models. *Atmos. Sci. Lett.* 7, 26–34.
- Yu, S., Dennis, R., Roselle, S., Nenes, A., Walker, J., Eder, B., Schere, K., Swall, J., Robarge, W., 2005. An assessment of the ability of 3-D air quality models with current thermodynamic equilibrium models to predict aerosol NO₃. *J. Geophys. Res.* 110, D07S13. <http://dx.doi.org/10.1029/2004JD004718>.
- Yu, S.-C., Mathur, R., Pleim, J., Wong, D., Gilliam, R., Alapaty, K., Zhao, C., Liu, X., 2014. Aerosol indirect effect on the grid-scale clouds in the two-way coupled WRF-CMAQ: model description, development, evaluation and regional analysis. *Atmos. Chem. Phys.* 14, 11247–11285. <http://dx.doi.org/10.5194/acp-14-11247-2014>.
- Zaveri, A.A., Peters, L.K., 1999. A new lumped structure photochemical mechanism for large-scale applications. *J. Geophys. Res.* 104, 30,387–30,415.

- Zender, C.S., Bian, H., Newman, D., 2003. Mineral dust entrainment and deposition (DEAD) model: description and 1990s dust climatology. *J. Geophys. Res.* 108 (D14), 4416. <http://dx.doi.org/10.1029/2002JD002775>.
- Zhang, D.F., Zakey, A.S., Gao, X.J., Giorgi, F., Solmon, F., 2009. Simulation of dust aerosol and its regional feedbacks over East Asia using a regional climate model. *Atmos. Chem. Phys.* 9, 1095–1110. <http://dx.doi.org/10.5194/acp-9-1095-2009>.
- Zhang, G.J., McFarlane, N.A., 1995. Sensitivity of climate simulations to the parameterization of cumulus convection in the Canadian Climate Centre general circulation model. *Atmos. Ocean.* 33, 407–446.
- Zhang, Q., Streets, D.G., He, K.-B., Wang, Y.-X., Richter, A., Burrows, J.P., Uno, I., Jang, C.J., Chen, D., Yao, Z.-L., Lei, Y., 2007. NO_x emission trends for China, 1995–2004: the view from the ground and the view from space. *J. Geophys. Res.* 112, D22306. <http://dx.doi.org/10.1029/2007JD008684>.
- Zhang, Q., Streets, D.G., Carmichael, G.R., He, K.-B., Huo, H., Kannari, A., Klimont, Z., Park, I.S., Reddy, S., Fu, J.-S., Chen, D., Duan, L., Lei, Y., Wang, L.-T., Yao, Z.-L., 2009. Asian emissions in 2006 for the NASA INTEX-B mission. *Atmos. Chem. Phys.* 9, 5131–5153. <http://dx.doi.org/10.5194/acp-9-5131-2009>.
- Zhang, Q., Quan, J., Tie, X., Huang, M., Ma, X., 2011. Impacts of aerosol particles on cloud formation: aircraft measurements in China. *Atmos. Environ.* 45, 665–672.
- Zhang, Y., Pun, B., Vijayaraghavan, K., Wu, S.-Y., Seigneur, C., Pandis, S., Jacobson, M., Nenes, A., Seinfeld, J.H., 2004. Development and application of the model of aerosol dynamics, reaction, ionization and dissolution (MADRID). *J. Geophys. Res.* 109, D01202. <http://dx.doi.org/10.1029/2003JD003501>.
- Zhang, Y., Liu, P., Pun, B., Seigneur, C., 2006. A comprehensive performance evaluation of MM5-CMAQ for summer 1999 Southern Oxidants Study episode, Part I. Evaluation protocols, databases, and meteorological predictions. *Atmos. Environ.* 40, 4825–4838.
- Zhang, Y., Vijayaraghavan, K., Wen, X.-Y., Snell, H.E., Jacobson, M.Z., 2009. Probing into regional ozone and particulate matter pollution in the United States: 1. A 1-year CMAQ simulation and evaluation using surface and satellite data. *J. Geophys. Res.* 114, D22304. <http://dx.doi.org/10.1029/2009JD011898>.
- Zhang, Y., Wen, X.-Y., Jang, C.J., 2010. Simulating chemistry-aerosol-cloud-radiation-climate feedbacks over the Continental U.S. using the online-coupled Weather Research Forecasting model with chemistry (WRF/Chem). *Atmos. Environ.* 44 (29), 3568–3582.
- Zhang, Y., Karamchandani, P., Glotfelty, T., Streets, D.G., Grell, G., Nenes, A., Yu, F., Bennartz, R., 2012a. Development and initial application of the global-through-urban weather research and forecasting model with chemistry (GU-WRF/Chem). *J. Geophys. Res.* 117, D20206. <http://dx.doi.org/10.1029/2012JD017966>.
- Zhang, Y., Chen, Y.-C., Sarwar, G., Schere, K., 2012b. Impacts of gas-phase mechanisms on weather research forecasting model with chemistry (WRF/Chem) predictions: mechanism implementation and comparative evaluation. *J. Geophys. Res.* 117, D01301. <http://dx.doi.org/10.1029/2011JD015775>.
- Zhang, Y., Zhang, X., Wang, K., He, J., Leung, L.R., Fan, J., Nenes, A., 2015a. Incorporating an advanced aerosol activation parameterization into WRF-CAM5: model evaluation and parameterization intercomparison. *J. Geophys. Res. Atmos.* 120, 6952–6979. <http://dx.doi.org/10.1002/2014JD023051>.
- Zhang, Y., Chen, Y., Fan, J.-W., Leung, L.-Y.R., 2015b. Application of an online-coupled regional climate model, WRF-CAM5, over East Asia for examination of ice nucleation schemes: Part II. Sensitivity to heterogeneous ice nucleation parameterizations and dust emissions. *Climate* 3, 753–774. <http://dx.doi.org/10.3390/cli3030753>.
- Zhang, Y., Zhang, X., Wang, L.-T., Zhang, Q., Duan, F., He, K.-B., 2016a. Application of WRF/chem over east Asia: Part I. Model evaluation and intercomparison with MM5/CMAQ. *Atmos. Environ.* 124, 285–300. <http://dx.doi.org/10.1016/j.atmosenv.2015.07.022>.
- Zhang, Y., Zhang, X., Wang, K., Zhang, Q., Duan, F., He, K.-B., 2016b. Application of WRF/Chem over East Asia: Part II. Model improvement and sensitivity simulations. *Atmos. Environ.* 124, 301–320. <http://dx.doi.org/10.1016/j.atmosenv.2015.07.023>.
- Zhang, Y., 2008. Online-coupled meteorology and chemistry models: history, current status, and outlook. *Atmos. Chem. Phys.* 8, 2895–2932. <http://dx.doi.org/10.5194/acp-8-2895-2008>.
- Zhuang, B.-L., Li, S., Wang, T.-J., Deng, J.-J., Xie, M., Yin, C.-Q., Zhu, J.-L., 2013. Direct radiative forcing and climate effects of anthropogenic aerosols with different mixing states over China. *Atmos. Environ.* 79, 349–361. <http://dx.doi.org/10.1016/j.atmosenv.2013.07.004>.
- Ziemke, J.R., Chandra, S., Duncan, B.N., Froidevaux, L., Bhartia, P.K., Levelt, P.F., Waters, J.W., 2006. Tropospheric ozone determined from Aura OMI and MLS: evaluation of measurements and comparison with the global modeling Initiative's chemical transport model. *J. Geophys. Res.* 111, D19303. <http://dx.doi.org/10.1029/2006JD007089>.